Supplementary Information for

IL-4 Drives Exhaustion in CD8⁺ CART Cells

Authors: Carli M. Stewart[1,2,3], Elizabeth L. Siegler[1,4], R. Leo Sakemura[1,4] , Michelle J. Cox[1], Truc Huynh[1,4], Brooke Kimball[1,4], Long Mai[1,4], Ismail Can[1,4],Claudia Manriquez Roman[1] , Kun Yun[1,2,5], Olivia Sirpilla[1,2,3], James H. Girsch[1,2,5], Ekene Ogbodo[1,4], Wazim Ismail[6], Alexandre Gaspar Maia[6,], Justin Budka[7], Jenny Kim[7], Nathalie Scholler[7], Mike Mattie[7], Simone Filosto[7], and Saad S. Kenderian[1,4,8*]

[1]T Cell Engineering, Mayo Clinic, Rochester, MN, USA
[2]Mayo Clinic Graduate School of Biomedical Sciences, Mayo Clinic, Rochester, MN, USA
[3]Department of Molecular Pharmacology and Experimental Therapeutics, Mayo Clinic, Rochester, MN, USA
[4]Division of Hematology, Mayo Clinic, Rochester, MN, USA
[5]Department of Molecular Medicine, Mayo Clinic, Rochester, MN, USA
[6]Department of Lab Medicine and Pathology, Mayo Clinic, Rochester, MN, USA
[7]Department of Oncology, Gilead Sciences Inc., Foster City, CA, USA
[8]Department of Immunology, Mayo Clinic, Rochester, MN, USA
*kenderian.saad@mayo.edu

TABLES

Table S1: **Antibodies used for flow cytometry experiments in this study.**

Antibody Name	Clone	Vendor	Catalog #	Assay
CD3, α-Hu APC-Cy7	SK7	BioLegend	344818	Proliferation and Inhibitory Receptor Expression
CD3, α-Hu APC	UCHT1	eBioscience	17-0038-42	Intracellular Cytokine Production
CD3, α-Hu BV605	SK7	BioLegend	344836	In vivo Blood and Organ Processing
CD4, α-Hu BV785	OKT4	BioLegend	317442	In vivo Blood and Organ Processing
CD4, α-Hu FITC	OKT4	eBioscience	11-0048-42	Th1 vs. Th2
CD8, α-Hu PerCP	SK1	BioLegend	344708	All panels
CD20, α-Hu PerCP	2H7	BioLegend	302324	In vivo Blood and Organ Processing
CD20, α-Hu APC	2H7	BioLegend	302310	In vivo Blood Processing
CD45, α-Mouse APC-eFluor780	30-F11	eBioscience	47-0451-82	In vivo Blood and Organ Processing
CD45, α-Hu BV421	HI30	BioLegend	304032	In vivo Blood and Organ Processing
IL-2, α-Hu PE-CF594	5344.111	BD Biosciences	562384	Intracellular Cytokine Production
IL-4, α-Hu APC	MP4-25D2	BD Biosciences	554486	Intracellular Cytokine Production
IL4R, α-Hu APC	G077F6	BioLegend	355005	IL4R Expression Check

TNF-α, α-Hu AF700	MAb11	BioLegend	502928	Intracellular Cytokine Production
IFN-γ, α-Hu APC-efluor 780	4S.B3	eBioScience	47-7319-42	Intracellular Cytokine Production
GM-CSF, α-Hu BV421	BVD2-21C11	BD Biosciences	562930	Intracellular Cytokine Production
PD-1, α-Hu BV-421	EH12.2H7	BioLegend	329920	In vitro Inhibitory Receptor Expression
PD-1, α-Hu FITC	MIH4	eBioscience	11-9969-42	In vivo Blood and Organ Processing
TIM-3, α-Hu PE	F38-2E2	BioLegend	345006	Inhibitory Receptor Expression
CTLA-4, α-Hu PE-Cy7	BNI3	BioLegend	369614	In vitro Inhibitory Receptor Expression
LAG-3, α-Hu FITC	3DS223H	eBioscience	11-2239-42	In vitro Inhibitory Receptor Expression
CCR4, α-Hu PerCP	L291H4	BioLegend	359406	Th1 vs. Th2
CCR6, α-Hu APC	11A9	BD Biosciences	560619	Th1 vs. Th2
CXCR3, α-Hu APC-Cy7	G02H7	BioLegend	353722	Th1 vs. Th2
Live/Dead Aqua	N/A	Invitrogen	L34966	All Panels
Biotin Protein L (Primary Antibody)	N/A	GenScript	M00097	CAR Detection
Streptavidin, PE (Secondary Antibody)	N/A	BioLegend	405203	CAR Detection

Table S2: **Primers used for CRISPR screen library preparation.**

Primer Name	Sequence
NGS-Lib-Fwd-1	AATGATACGGCGACCACCGAGATCTA CACTCTTTCCCTACACGACGCTCTTCC GATCTTAAGTAGAGGCTTTATATATCT TGTGGAAAGGACGAAACACC
NGS-Lib-Fwd-2	AATGATACGGCGACCACCGAGATCTA CACTCTTTCCCTACACGACGCTCTTCC GATCTATCATGCTTAGCTTTATATATC TTGTGGAAAGGACGAAACACC
NGS-Lib-Fwd-3	AATGATACGGCGACCACCGAGATCTA CACTCTTTCCCTACACGACGCTCTTCC GATCTGATGCACATCTGCTTTATATAT CTTGTGGAAAGGACGAAACACC
NGS-Lib-Fwd-4	AATGATACGGCGACCACCGAGATCTA CACTCTTTCCCTACACGACGCTCTTCC GATCTCGATTGCTCGACGCTTTATATA TCTTGTGGAAAGGACGAAACACC
NGS-Lib-Fwd-5	AATGATACGGCGACCACCGAGATCTA CACTCTTTCCCTACACGACGCTCTTCC GATCTTCGATAGCAATTCGCTTTATAT ATCTTGTGGAAAGGACGAAACACC
NGS-Lib-Fwd-6	AATGATACGGCGACCACCGAGATCTA CACTCTTTCCCTACACGACGCTCTTCC GATCTATCGATAGTTGCTTGCTTTATA TATCTTGTGGAAAGGACGAAACACC
NGS-Lib-Fwd-7	AATGATACGGCGACCACCGAGATCTA CACTCTTTCCCTACACGACGCTCTTCC GATCTGATCGATCCAGTTAGGCTTTAT ATATCTTGTGGAAAGGACGAAACACC
NGS-Lib-Fwd-8	AATGATACGGCGACCACCGAGATCTA CACTCTTTCCCTACACGACGCTCTTCC GATCTCGATCGATTTGAGCCTGCTTTA TATATCTTGTGGAAAGGACGAAACAC C
NGS-Lib-Fwd-9	AATGATACGGCGACCACCGAGATCTA CACTCTTTCCCTACACGACGCTCTTCC GATCTACGATCGATACACGATCGCTTT ATATATCTTGTGGAAAGGACGAAACA CC
NGS-Lib-Fwd-10	AATGATACGGCGACCACCGAGATCTA CACTCTTTCCCTACACGACGCTCTTCC GATCTTACGATCGATGGTCCAGAGCTT TATATATCTTGTGGAAAGGACGAAAC ACC
NGS-Lib-KO-Rev-1	CAAGCAGAAGACGGCATACGAGATTC GCCTTGGTGACTGGAGTTCAGACGTG TGCTCTTCCGATCTCCGACTCGGTGCC ACTTTTTCAA
NGS-Lib-KO-Rev-2	CAAGCAGAAGACGGCATACGAGATAT AGCGTCGTGACTGGAGTTCAGACGTG TGCTCTTCCGATCTCCGACTCGGTGCC ACTTTTTCAA
NGS-Lib-KO-Rev-3	CAAGCAGAAGACGGCATACGAGATGA AGAAGTGTGACTGGAGTTCAGACGTG TGCTCTTCCGATCTCCGACTCGGTGCC ACTTTTTCAA

Table S3. **Cycling Conditions for CRISPR screen library preparation.**

Cycle Number	Denature	Anneal	Extend
1	98°C, 3 minutes		
2-23	98°C, 10 seconds	63°C, 10 seconds	72°C, 25 seconds
24			72°C, 2 minutes

SUPPLEMENTARY FIGURES

Supplementary Figure S1

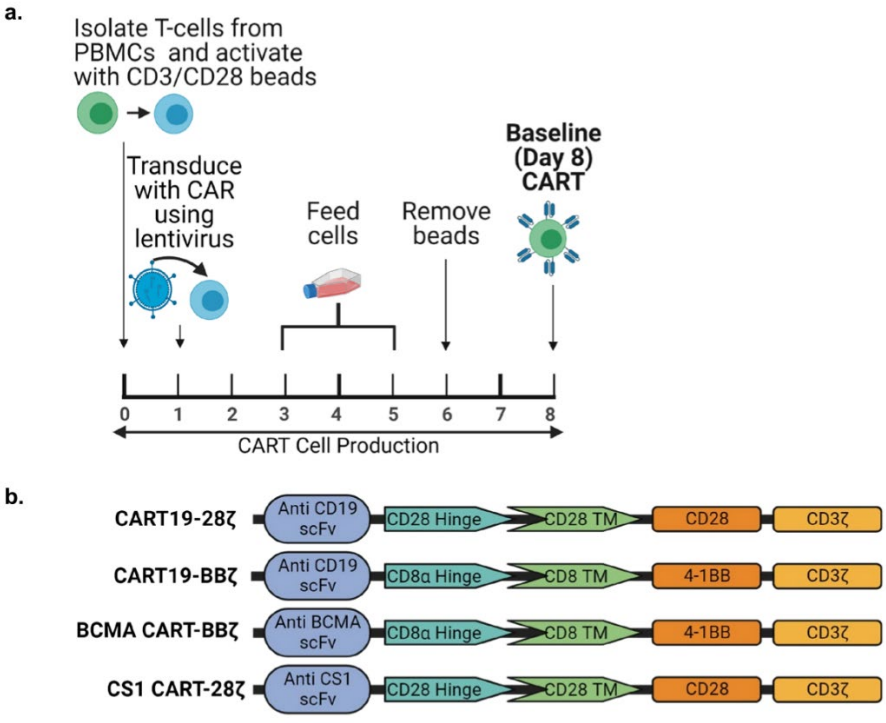

Supplementary Figure S1. **Healthy donor CART cell production for in vitro and in vivo studies. a.** Schematic showing the CART cell production process for lentivirally transduced CART cells. **b.** Schematic describing the modular domains included in the lentivirally transduced CART cells used in in vitro and in vivo validation studies (scFv = single-chain variable fragment, TM = transmembrane). (Supplementary Figure S1a-b was created with BioRender.com released under a Creative Commons Attribution-NonCommercial-NoDerivs 4.0 International license)

Supplementary Figure S2

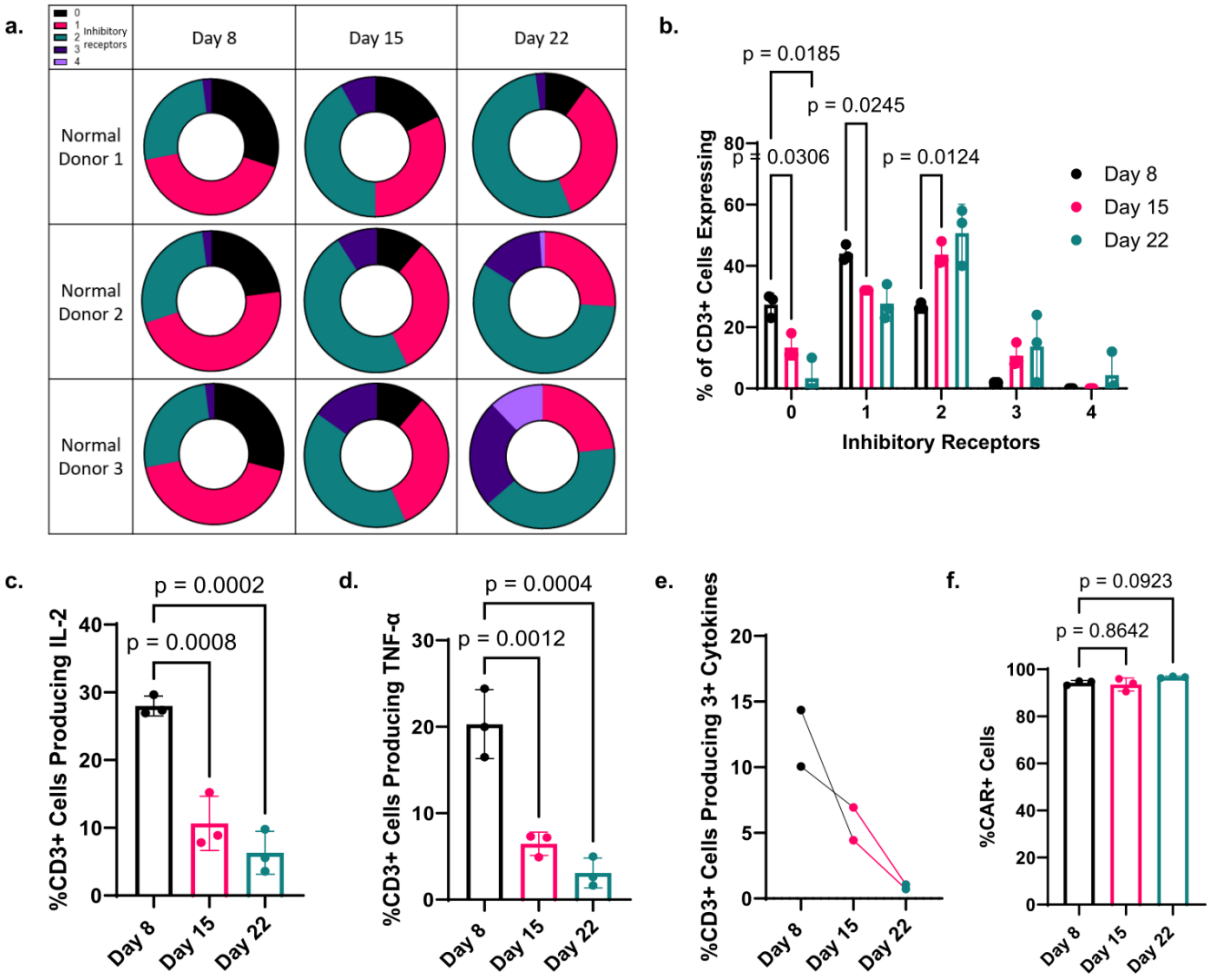

Supplementary Figure S2. **CART19-28ζ cells chronically stimulated by JeKo-1 target cells using the in vitro model for exhaustion show phenotypical and functional signs of**

exhaustion. a. Circle plot showing the percent of CART cells expressing multiple inhibitory receptors (0 – black, 1 – pink, 2- green, 3 – dark purple, 4 – light purple) over time as determined with flow cytometric detection of $CD3^+$ cells positive for PD-1, TIM-3, CTLA-4, and/or LAG-3 on Days 8, 15, and 22 of the in vitro model for exhaustion where CART19-28ζ cells were chronically stimulated with JeKo-1 target cells. **b.** Bar graph quantifying the circle plots in **a.** (Two-way ANOVA, average of two technical replicates for three biological replicates, mean +/- SD). **c-d.** The percent of CART19-28ζ cells producing the effector cytokines IL-2 and TNF-α, respectively, on Day 8, 15, and 22. This was determined by strongly stimulating CART cells at a 1:5 E:T cell ratio for four hours before performing intracellular staining for the cytokines (One-way ANOVA, average of two technical replicates for three biological replicates, mean +/- SD). **e.** The percent of CART19-28ζ cells producing three or more cytokines after strongly stimulating them at a 1:5 E:T cell ratio on Days 8, 15, and 22 of the in vitro model for exhaustion before performing intracellular staining for the following cytokines: IL-2, TNF-α, IFN-γ, and GM-CSF (Data from two biological replicates, two technical replicates per biological replicate). **f.** The percent of CAR^+ cells on Days 8, 15, and 22 of the in vitro model for exhaustion as determined with ProteinL staining and flow cytometry (One-way ANOVA, average of two technical replicates for three biological replicates, mean +/- SD). Source data are provided as a Source Data file.

Supplementary Figure S3

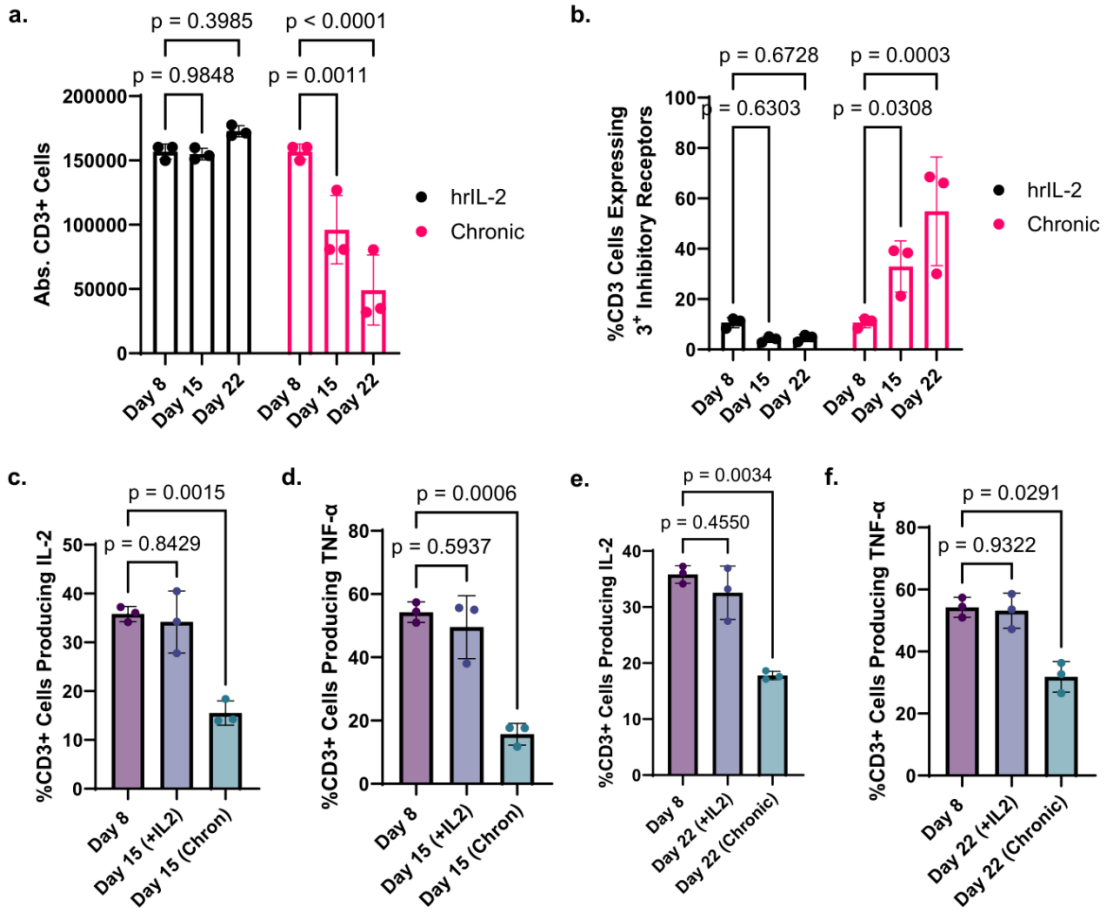

Supplementary Figure S3. **Long-term co-culture of CART cells in media supplemented with hrIL-2 does not result in dysfunction. a.** Absolute $CD3^+$ cell count after 100,000 CART cells were co-cultured with JeKo-1 cells at 1:1 E:T cell ratio for 5-days. Day 15 (hrIL-2) and Day 22 (hrIL-2) cells were kept in media supplemented with 100 IU/mL hrIL-2 from Day 8 to Day 15/Day 22 while Day 15 (Chronic) and Day 22 (Chronic) cells where chronically stimulated from Day 8 to Day 15/Day 22 according to the in vitro model for exhaustion. (Two-way ANOVA, average of two technical replicates for three biological replicates, mean +/- SD). **b.** The percent of either Day 8, Day 15 (hrIL-2), Day 22 (hrIL-2), Day 15 (Chronic), or Day 22 (Chronic) cells that express 0, 1, 2, 3, or 4 inhibitory receptors as determined by flow cytometric detection of $CD3^+$ cells positive for PD-1, TIM-3, CTLA-4, and LAG-3 (Two-way ANOVA, average of two technical replicated for three biological replicates, mean +/- SD). **c-f.** The percent of $CD3^+$ cells producing IL-2 and TNF-α after either Day 8, Day 15 (hrIL-2), Day 22 (hrIL-2), Day 15 (Chronic), or Day 22 (Chronic) cells were co-cultured with JeKo-1 cells at a 1:5 E:T ratio for 4 hours as determined with intracellular staining

for flow cytometry (One-way ANOVA, average of two technical replicates for three biological replicates, mean +/- SD) Source data are provided as a Source Data file.

Supplementary Figure S4

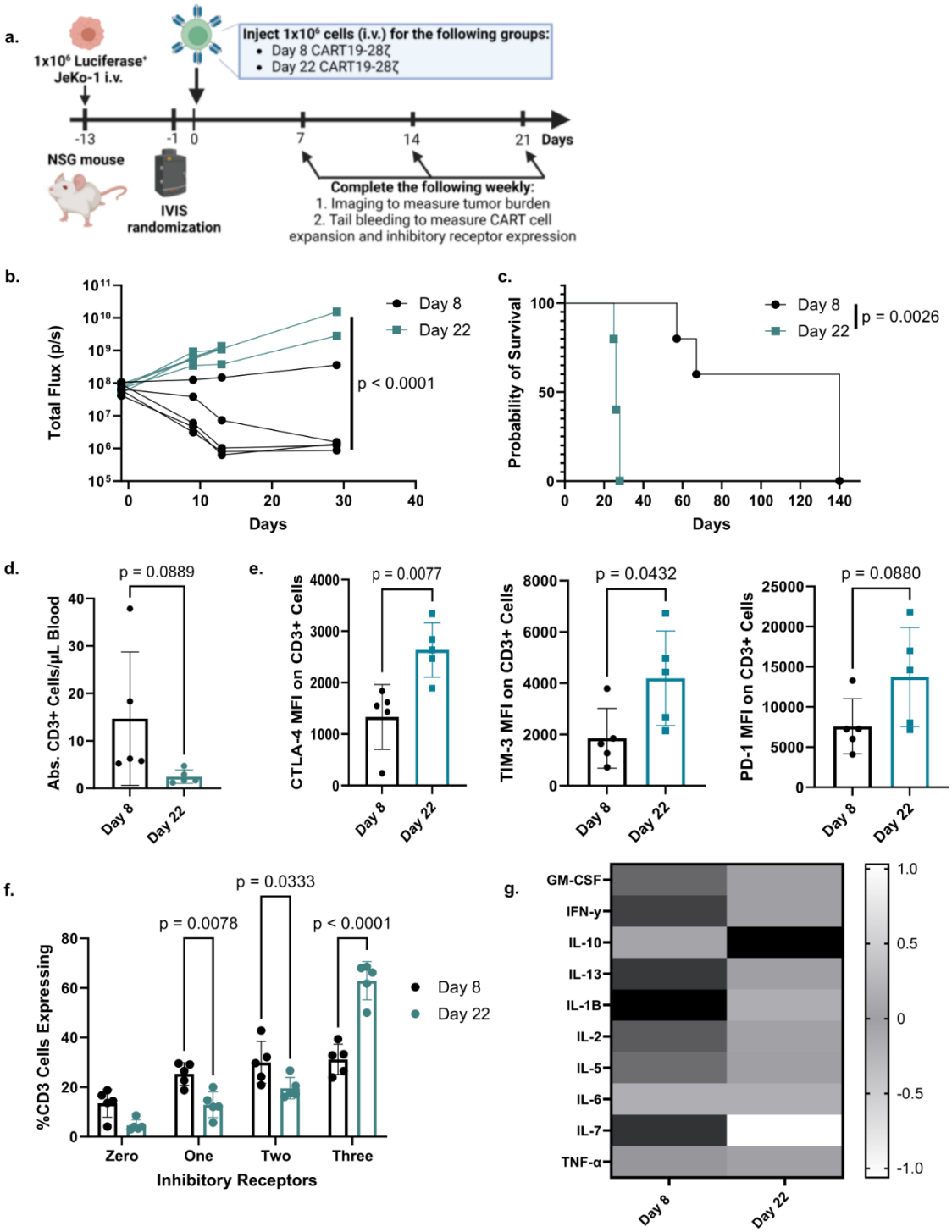

Supplementary Figure S4. **Day 22 CART19-28ζ cells from the in vitro model for exhaustion showed reduced overall efficacy in two separate mantle cell lymphoma xenograft mouse models with different T cell donors. a.** Schematic depicting an in vivo mantle cell lymphoma xenograft mouse model to induce stress in CART19 cells (Supplementary Figure S4a was created with BioRender.com released under a Creative Commons Attribution-NonCommercial-NoDerivs 4.0 International license). **b.** Tumor burden over time in a mantle cell lymphoma xenograft mouse model as determined by bioluminescence imaging of the luciferase^{+} tumor (Two-way ANOVA, n=5 mice per group, results from replicate experiment). **c.** Overall survival curve of mice in a mantle cell lymphoma xenograft mouse model (Log-rank (Mantel-Cox) test, n=5 mice per group, results from replicate experiment). **d.** Absolute human CD3^{+} cells per µL of peripheral blood as determined by flow cytometry on Day 14 of a mantle cell lymphoma xenograft mouse model (two-sided t-test, n=5 mice per group, results from replicate experiment, mean +/- SD). **e.** Mean fluorescence intensity of the inhibitory receptors CTLA-4, TIM-3, and PD-1 on human CD3^{+} cells in the peripheral blood of mice treated with either Day 8 or Day 22 CART19-28ζ cells on Day 14 of a mantle cell lymphoma xenograft mouse model (two-sided t-test, n=5 mice per group, mean +/- SD, results from replicate experiment). **f.** The percent of CART19-28ζ cells expressing multiple inhibitory receptors on Day 15 of a mantle cell lymphoma xenograft mouse model. This was determined through tail vein bleeding and flow cytometric detection of human CD3^{+} cells that are positive for PD-1, TIM-3, and/or CTLA-4 (Two-way ANOVA, n=5 mice per group, mean +/- SD). **g.** Heat map showing median of normalized values for cytokine concentration from each group of mice in the mantle cell lymphoma xenograft mouse model treated with either Day 8 or Day 22 CART19-28ζ cells (n=5 mice per group). Source data are provided as a Source Data file.

Supplementary Figure S5

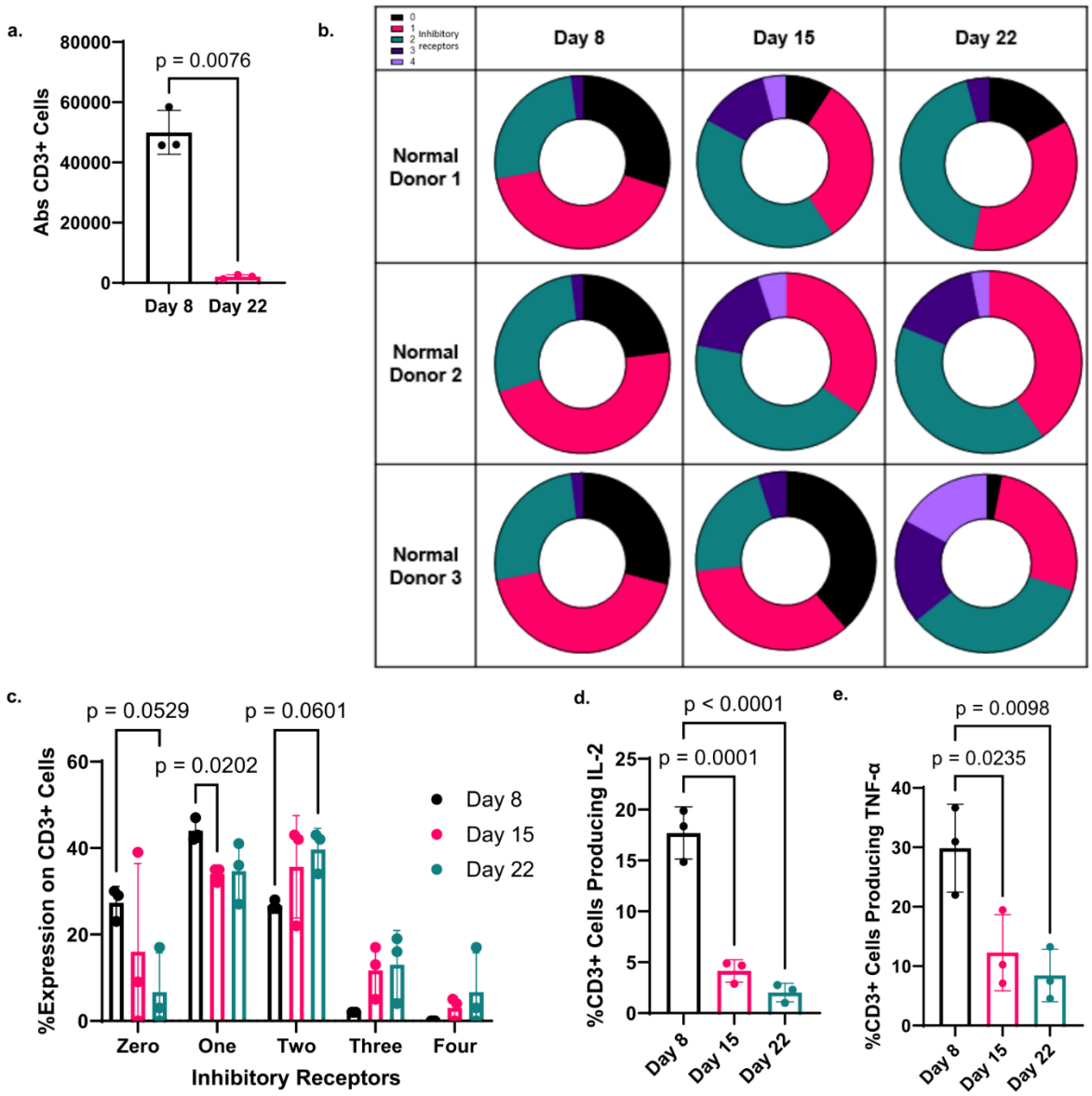

Supplementary Figure S5. **Chronic stimulation of CART19-28ζ cells with the CD19^{+} acute lymphoblastic leukemia (ALL) cell line, NALM6, using the in vitro model for exhaustion results in phenotypical and functional signs of exhaustion.** **a.** The absolute count of CD3^{+} T cells as determined with flow cytometry following co-culture of either Day 8 or Day 22 CART19-28ζ cells with NALM6 target cells at a 1:1 E:T cell ratio for 5-days (two-sided t-test , average of two technical replicates for three biological replicates, mean +/- SD). **b.** Circle plot showing the

percent of CART cells expressing multiple inhibitory receptors (0 – black, 1 – pink, 2- green, 3 – dark purple, 4 – light purple) over time as determined with flow cytometric detection of $CD3^+$ cells positive for PD-1, TIM-3, CTLA-4, and/or LAG-3 on Days 8, 15, and 22 of the in vitro model for exhaustion where CART19-28ζ cells were chronically stimulated with NALM6 target cells. **c.** Bar graph quantifying the circle plots in **b.** (Two-way ANOVA, average of two technical replicates for three biological replicates, mean +/- SD). **d-e.** The percent of $CD3^+$ cells producing IL-2 and TNF-α as determined with intracellular staining and flow cytometry after either Day 8, Day 15, or Day 22 CART19-28ζ cells were co-cultured with NALM-6 cells at a 1:5 E:T cell ratio for four hours (One-way ANOVA, average of two technical replicates for three biological replicates, mean +/- SD). Source data are provided as a Source Data file.

Supplementary Figure S6

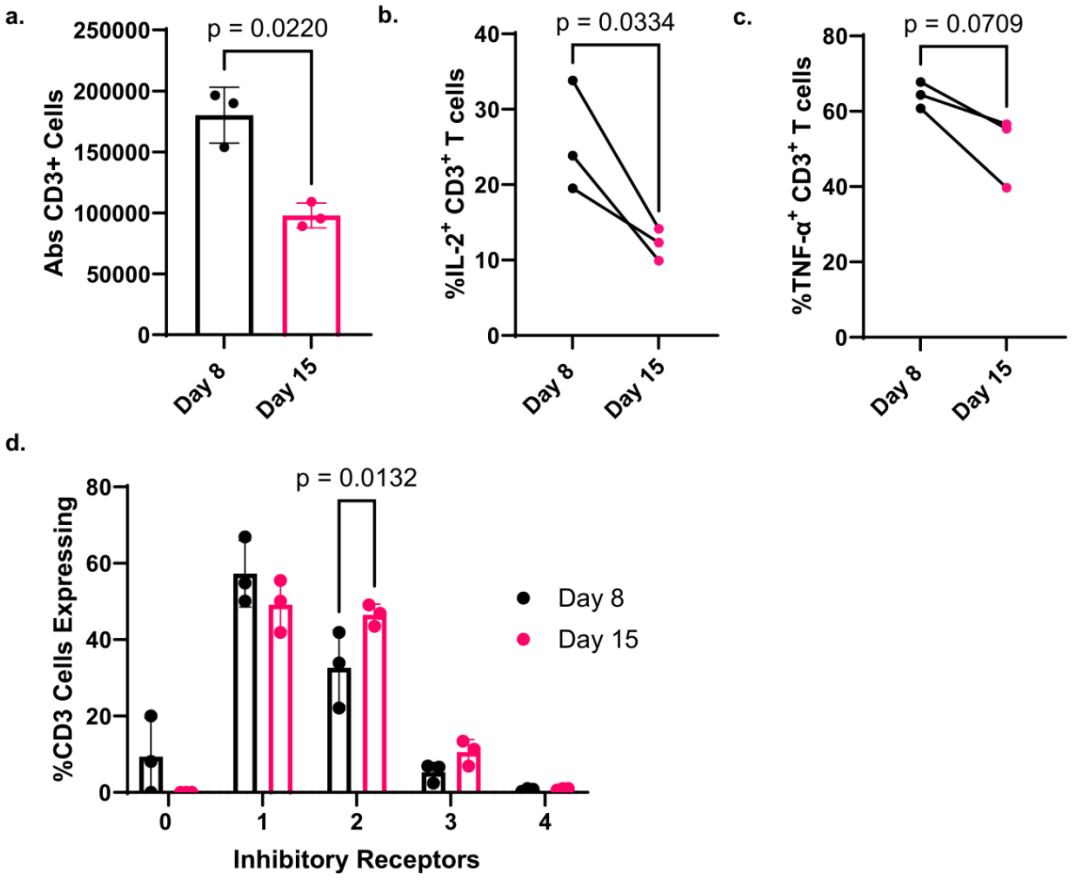

Supplementary Figure S6. **Chronic stimulation of CART19-BBζ cells with CD19$^+$ JeKo-1 cells using the in vitro model for exhaustion results in phenotypic and functional signs of exhaustion. a.** Absolute CD3$^+$ count as determined with flow cytometry after culturing either Day 8 or Day 15 CART19-BBζ cells with JeKo-1 cells for 5-days at a 1:1 E:T cell ratio (Paired t-test, average of two technical replicates for three biological replicates, mean +/- SD). **b-c.** The percent of CART19-BBζ cells producing either IL-2 or TNF-α as determined by intracellular staining for flow cytometry after stimulating either Day 8 or Day 15 CART cells at a 1:5 E:T ratio for four hours (Paired t-test, average of two technical replicates for three biological replicates). **d.** The percent of CART19-BBζ cells positive for either 0, 1, 2, 3, or 4 inhibitory receptors as determined with flow cytometry on Day 8 and Day 15 of the in vitro model for exhaustion after staining for PD-1, TIM-3, CTLA-4, and LAG-3 (Two-way ANOVA, average of two technical replicates for three biological replicates, mean +/- SD). Source data are provided as a Source Data file.

Supplementary Figure S7

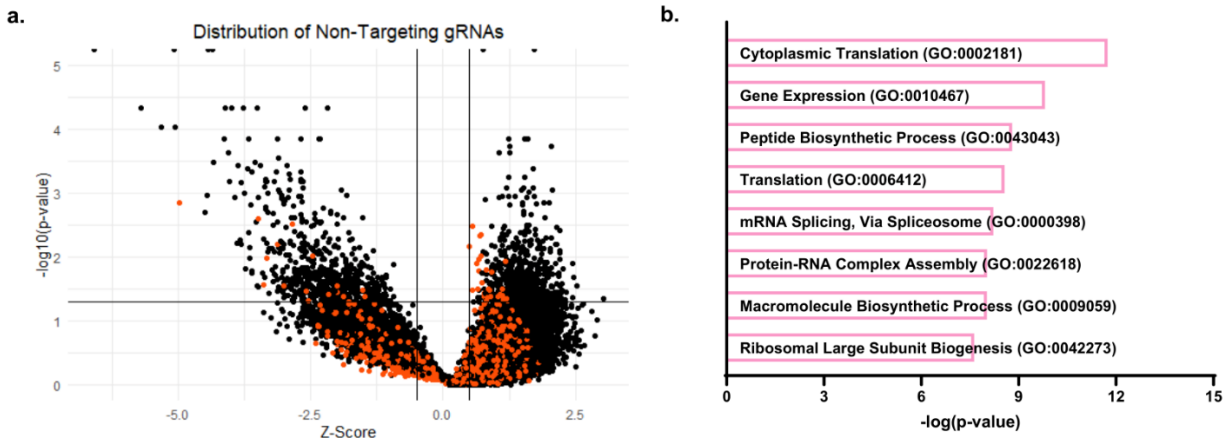

Supplementary Figure S7. **Plots to determine quality of the genome-wide CRISPR screen**. **a.** Volcano plot showing the distribution of positively and negatively selected gRNAs in the genome-wide CRISPR screen by Day 22 as compared to Day 8. Red dots represent the 1,000 non-targeting gRNAs utilized in the screen (three biological replicates, MAGeCK-VISPR MLE analysis). **b.** Gene set enrichment analysis of negatively selected genes (FDR<0.25) by Day 22

of the genome-wide CRISPR knockout screen (three biological replicates, MAGeCK-VISPR MLE analysis and normalization to the list of non-targeting gRNAs).

Supplementary Figure S8

a.

	Molecule Type	P-Value
LARP1	Translation Regulator	3.85E-12
PA2G4	Transcription Regulator	1.88E-14
IL4R	Transmembrane Receptor	3.51E-14
CCNG1		3.84E-14
MLXIPL	Transcription Regulator	5.70E-14

b.

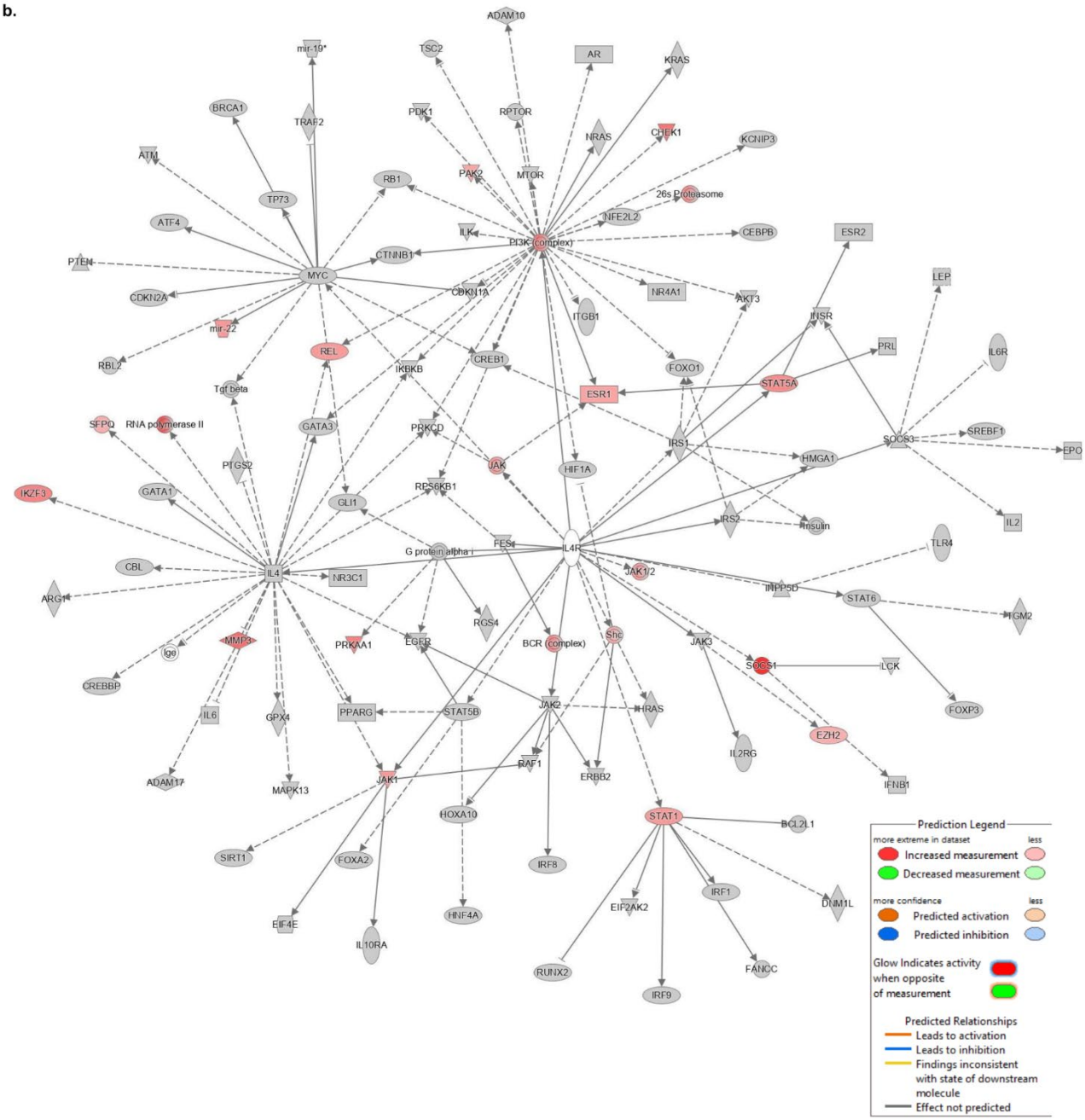

Supplementary Figure S8. **Ingenuity pathway analysis of positively selected genes in the genome-wide CRISPR knockout screen. a.** Top five causal networks identified through analysis of genes that were positively selected for by Day 22 of the genome-wide CRISPR knockout screen. **b.** QIAGEN IPA network for IL4R and affected genes as identified in the list of positively selected genes. (Positive selection in the CRISPR screen was defined as FDR<0.25 with MAGeCK-VISPR MLE analysis)

Supplementary Figure S9

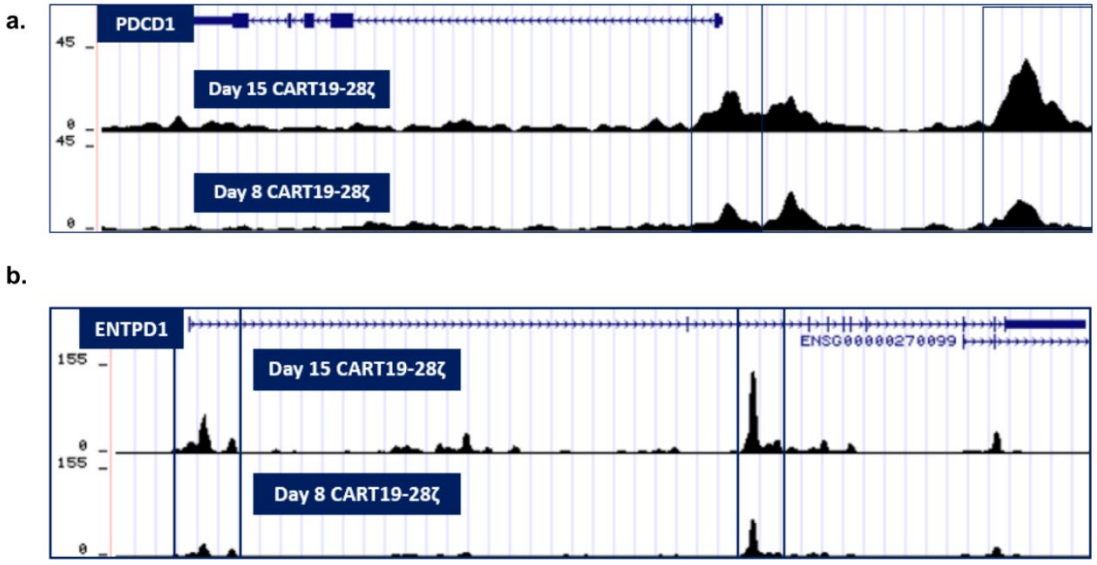

Supplementary Figure S9. **Chromatin accessibility interrogation of baseline and chronically stimulated CART19-28ζ cells from the in vitro model for exhaustion reveal key epigenetic signatures of exhaustion. a-b.** ATAC signal track of selected gene loci (*PDCD1* and *ENTPD1*) showing averaged signal for the three biological replicates at each timepoint as visualized with the UCSC genome browser.

Supplementary Figure S10

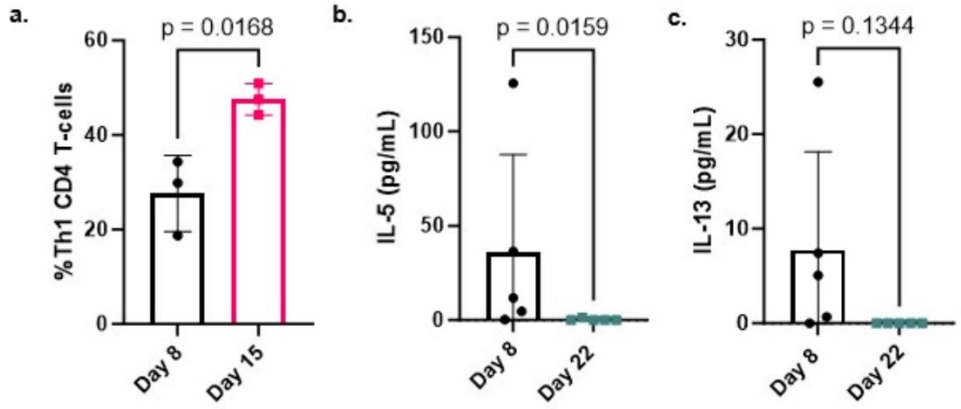

Supplementary Figure S10. **Changes in the Th1/Th2 pathway during the in vitro model for exhaustion. a.** The percent of Th1 $CD4^+$ CART19-28ζ cells as defined by $CCR6^-CCR4^-CXCR3^+$ cells by flow cytometry (t-test, average of two technical replicates for three biological replicates, mean +/- SD). **b-c.** The concentration of IL-5 and IL-13 in the serum by Multiplex assay of JeKo-1 xenograft mice two weeks after the injection of either Day 8 or Day 22 CART19-28ζ cells (two-sided t-test, n=5 mice per group, mean +/- SD). Source data are provided as a Source Data file.

Supplementary Figure S11

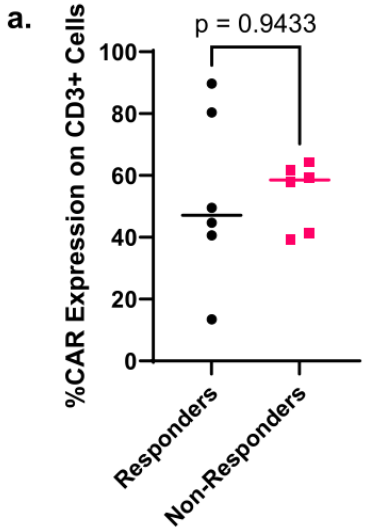

Supplementary Figure S11. **No difference in CAR^+ T cells in the pre-infusion products from responders and non-responders in the ZUMA-1 clinical trial. a.** The percent of $CD3^+$ cells

expressing CAR as determined by positive staining for an anti-Whitlow linker antibody using flow cytometry. (two-sided t-test, n=6 responder and n=6 non-responder samples, median value) Source data are provided as a Source Data file.

Supplementary Figure S12

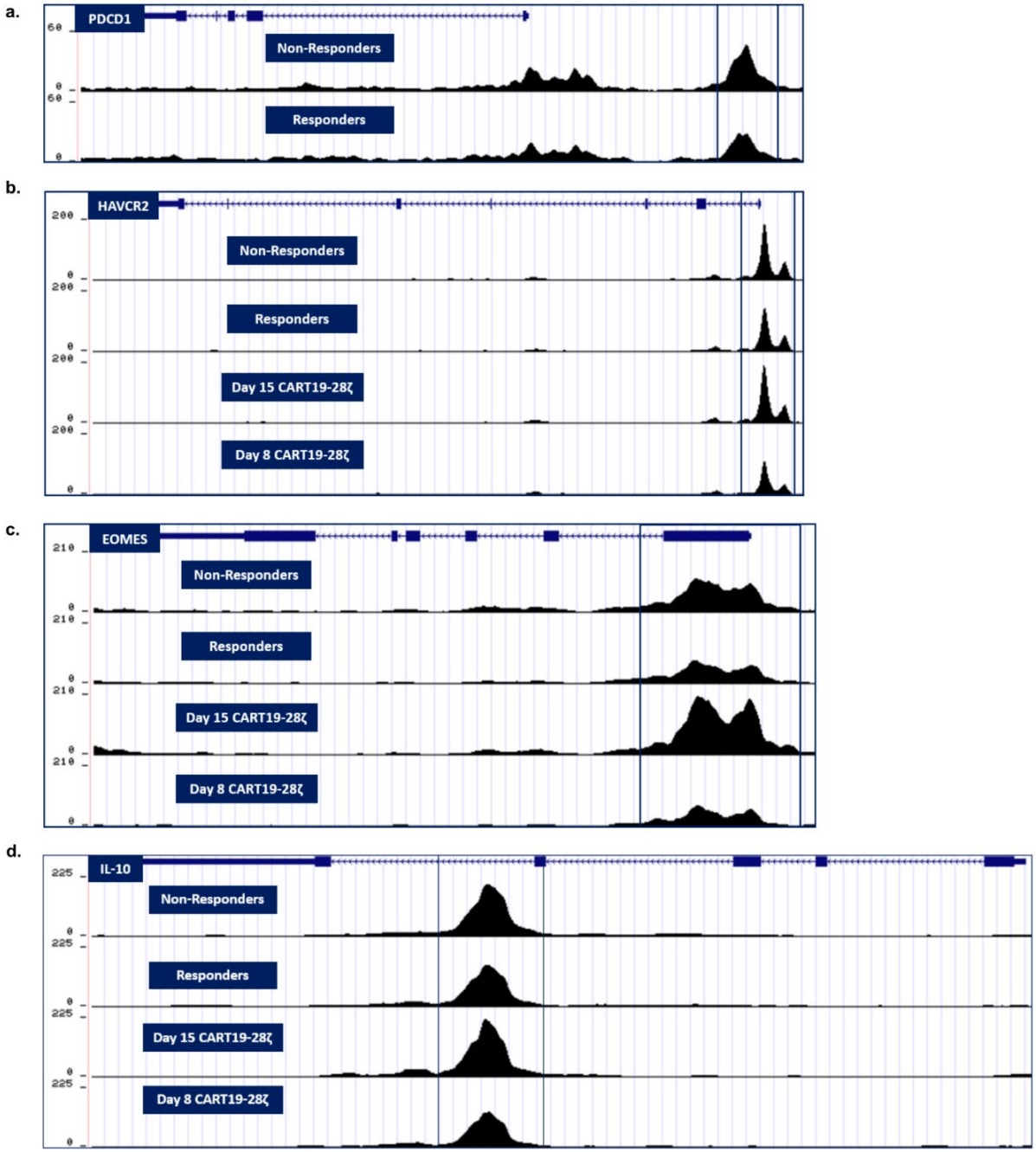

Supplementary Figure S12. **Chromatin accessibility analysis of pre-infusion axi-cel products from 6 responders and 6 non-responders in the ZUMA-1 clinical trial. a-d.** ATAC signal track of selected exhaustion-related gene loci (*PDCD1, HAVCR2* (TIM-3), *EOMES, IL-10*) based on averaged signal for the biological replicates for each condition (n=6 for responders and n=6 for non-responders; n=3 for Day 15 and n= 3 Day 8 CART29-28ζ).

Supplementary Figure S13

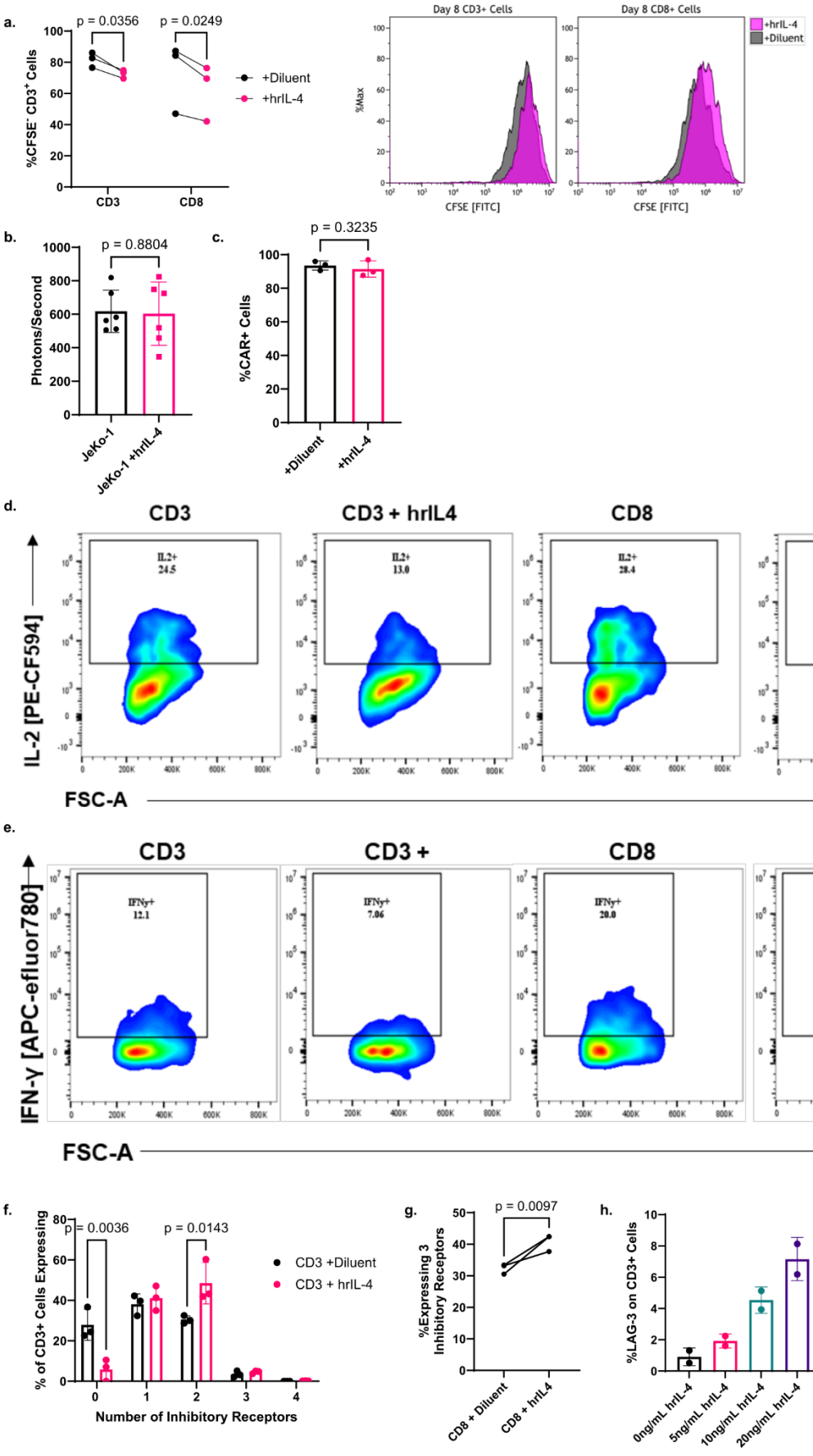

Supplementary Figure S13. **The effect of treatment with human recombinant IL-4 (hrIL-4) in vitro. a.** Line graph and representative histogram from one biological replicate showing the shift in CFSE staining as determined by flow cytometry after CFSE labeled bulk or $CD8^+$ CART cells were co-cultured with JeKo-1 tumor cells for 5-days (Two-way ANOVA, three biological replicates). **b.** The luminescence (photons/second) of $luciferase^+$ JeKo-1 cells after 48 hours of treatment with either diluent or 20ng/mL hrIL-4 (two-sided t-test, six technical replicates, mean +/- SD). **c.** The percent of CAR^+ cells following chronic stimulation (Day 15) in the presence of diluent or 20ng/mL hrIL-4 as determined with ProteinL staining for flow cytometry. (two-sided t-test, average of two technical replicates for three biological replicates, mean +/- SD) **d-e.** Representative flow plots showing the percent of $CD3^+$ cells producing IL-2 and IFN-γ as determined with intracellular staining and flow cytometry after Day 15 bulk or CD8+ CART19-28ζ cells, chronically stimulated in the presence of either diluent or 20ng/mL hrIL-4, were co-cultured with JeKo-1 cells at a 1:5 E:T cell ratio for four hours. **f.** The percent of $CD3^+$ cells expressing 0, 1, 2, 3, or 4 inhibitory receptors after bulk ($CD3^+$) CART19-28ζ cells were chronically stimulated with JeKo-1 cells in the presence of either diluent or 20ng/mL hrIL-4 from Day 8 to Day 15 of the in vitro model for exhaustion. Determined through flow cytometric staining for CD3, PD-1, CTLA-4, TIM-3, and LAG-3 (Two-way ANOVA, average of two technical replicates for three biological replicates, mean +/- SD). **g.** The percent of $CD3^+$ cells expressing 3 inhibitory receptors after isolated CD8 CART19-28ζ cells were kept in media supplemented with 100 IU/mL hrIL-4 and chronically stimulated in the presence of either diluent or 20ng/mL hrIL-4 from Day 8 to Day 15 of the in vitro model for exhaustion. Determined through flow cytometric staining for CD3, PD-1, CTLA-4, TIM-3, and LAG-3 (two-sided t-test, average of two technical replicates for three biological replicates). **h.** The percent of CART19-28ζ cells expressing the inhibitory receptor LAG-3 after one week of chronic stimulation with JeKo-1 cells in the presence of either 0, 5, 10, or

20ng/mL hrIL-4 (two technical replicates, one biological replicate). Source data are provided as a Source Data file.

Supplementary Figure S14

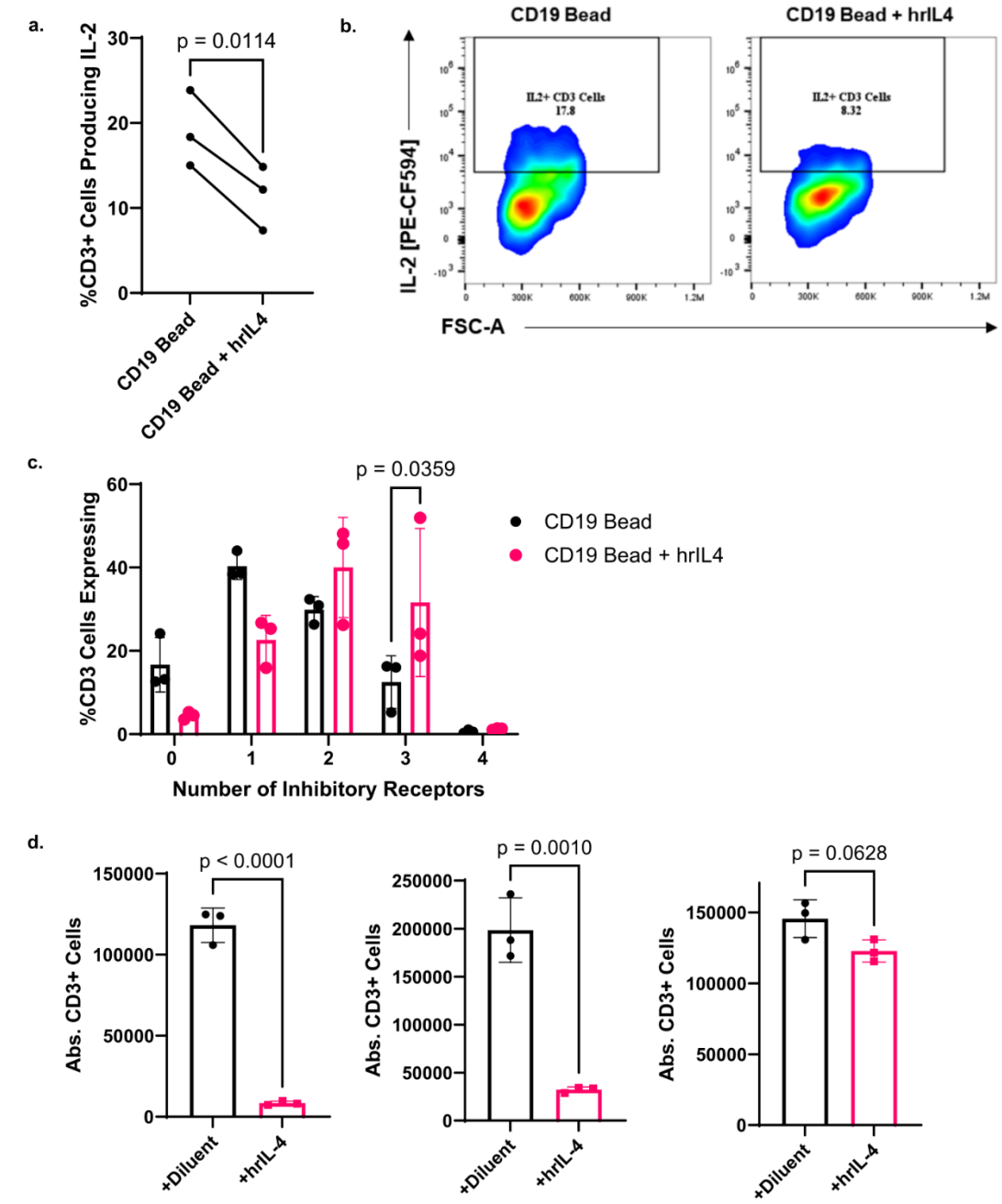

Supplementary Figure S14. **IL-4-driven CART cell exhaustion is independent of tumor cells.** **a-b.** Line graph and representative flow plots showing the percent of CART cells producing IL-2

following chronic stimulation from Day 8 to Day 15 with CD19 beads in the presence of either diluent or 20ng/mL hrIL-4. CART cell production of IL-2 was determined through intracellular staining for flow cytometry following four hours of co-culture with JeKo-1 cells at a 1:5 E:T ratio (Paired two-sided t-test, average of two technical replicates for three biological replicates). **c.** The percent of CART19-28ζ cells expressing 0, 1, 2, 3, or 4 inhibitory receptors after CART19-28ζ cells were chronically stimulated with CD19 beads either in the presence of diluent or 20ng/mL hrIL-4 from Day 8 to Day 15 of the in vitro model for exhaustion (Two-way ANOVA, average of two biological replicates for three biological replicates, mean +/- SD). **d.** Plots from three biological replicates comparing absolute $CD3^+$ count after CART cells that have been chronically stimulated from Day 8 to Day 15 in the presence of either diluent or hrIL-4 are co-cultured with JeKo-1 cells at a 1:1 E:T ratio for five days. (Unpaired two-sided t-test, three technical replicates per biological replicate, mean +/- SD). Source data are provided as a Source Data file.

Supplementary Figure S15

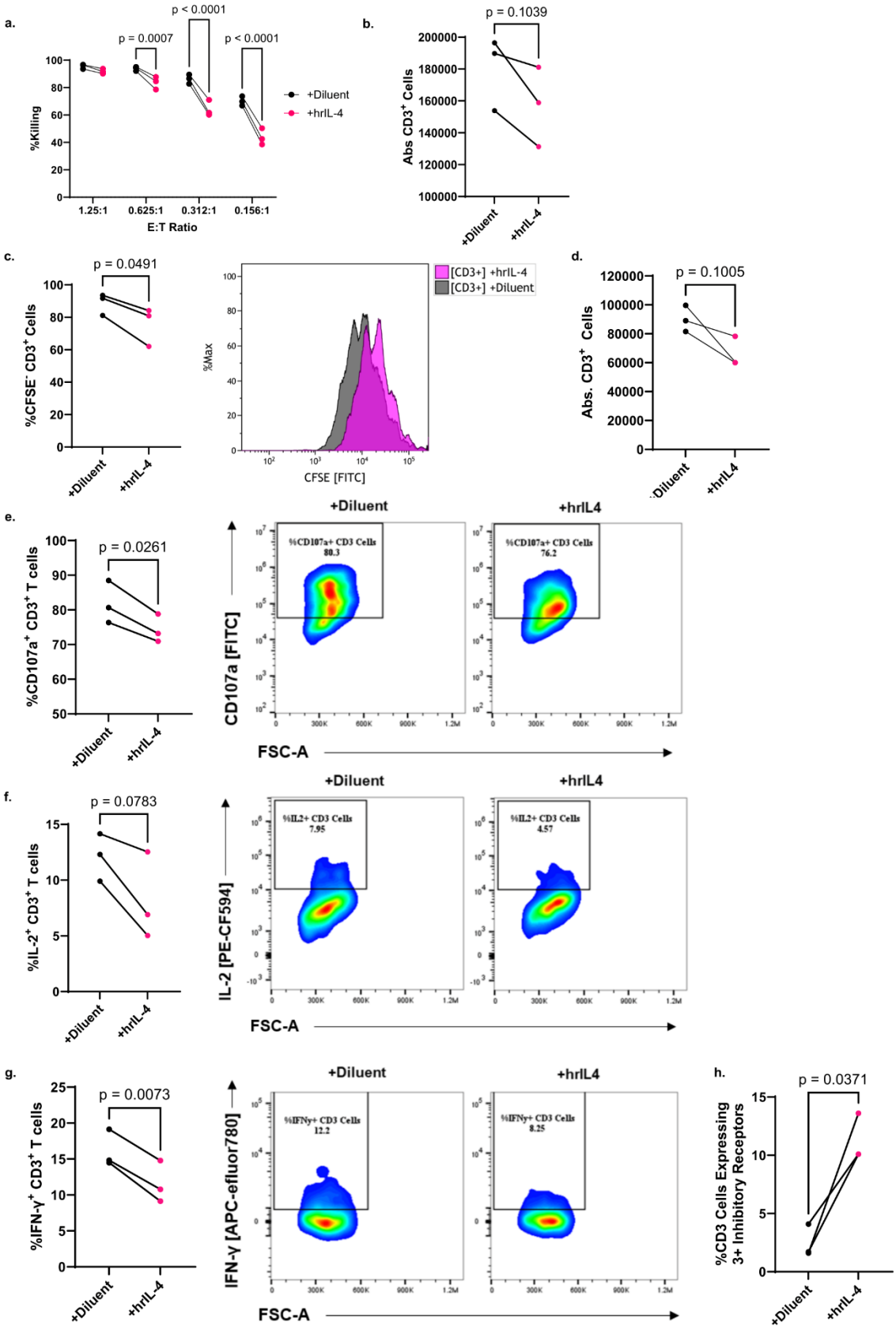

Supplementary Figure S15. **IL-4 drives exhaustion in CART19 cells containing a 4-1BB costimulatory domain (CART19-BBζ). a.** Percent killing as measured with bioluminescent imaging after Day 8 CART19-BBζ cells were co-cultured with luciferase^{+} JeKo-1 cells at various E:T cell ratios for 48 hours in the presence of either 20ng/mL human recombinant IL-4 (hrIL-4) or diluent (Two-way ANOVA, average of two technical replicates for three biological replicates). **b.** Absolute CD3^{+} cell count as measured with flow cytometry after Day 8 CART19-BBζ cells were co-cultured with JeKo-1 cells at a 1:1 E:T cell ratio for five days in the presence of either 20ng/mL hrIL-4 or diluent. (Paired two-sided t-test, average of two technical replicates for three biological replicates). **c.** Line graph and representative histogram showing the change in CFSE stained cells as determined by flow cytometry after CFSE^{+} Day 8 CART cells were co-cultured with JeKo-1 tumor cells for 5-days (Paired two-sided t-test, three biological replicates). **d.** Absolute CD3^{+} cell count as measured with flow cytometry after Day 15 CART19-BBζ cells were co-cultured with JeKo-1 cells at a 1:1 E:T cell ratio for five days. Day 15 CART cells were chronically stimulated in the presence of either 20ng/mL hrIL-4 or diluent (Paired two-sided t-test, average of two technical replicates for three biological replicates). **e.** Line graph and representative flow plot showing the percent of cells expressing CD107a after chronic stimulation from Day 8 to Day 15 in the presence of either 20ng/mL hrIL-4 or diluent. Measured with flow cytometry after co-culturing the Day 15 cells with JeKo-1 cells at a 1:5 E:T ratio for four hours (Paired two-sided t-test, average of two technical replicates for three biological replicates). **f-g.** Line graphs and representative flow plots showing the percent of CD3^{+} cells producing IL-2 and IFN-γ as determined with intracellular staining and flow cytometry after Day 15 CART19-BBζ cells, chronically stimulated in the presence of either diluent or 20ng/mL hrIL-4, were co-cultured with JeKo-1 cells at a 1:5 E:T cell ratio for four hours (Paired two-sided t-test, average of two technical replicates for three biological replicates). **h.** The percent of CD3^{+} cells expressing three or more inhibitory receptors after chronic stimulation from Day 8 to Day 22 in the presence of diluent or 20ng/mL of hrIL-4.

Measured with flow cytometry after staining for CD3, PD-1, CTLA-4, TIM-3, and LAG-3 (Paired two-sided t-test, average of two technical replicates for three biological replicates). Source data are provided as a Source Data file.

Supplementary Figure S16

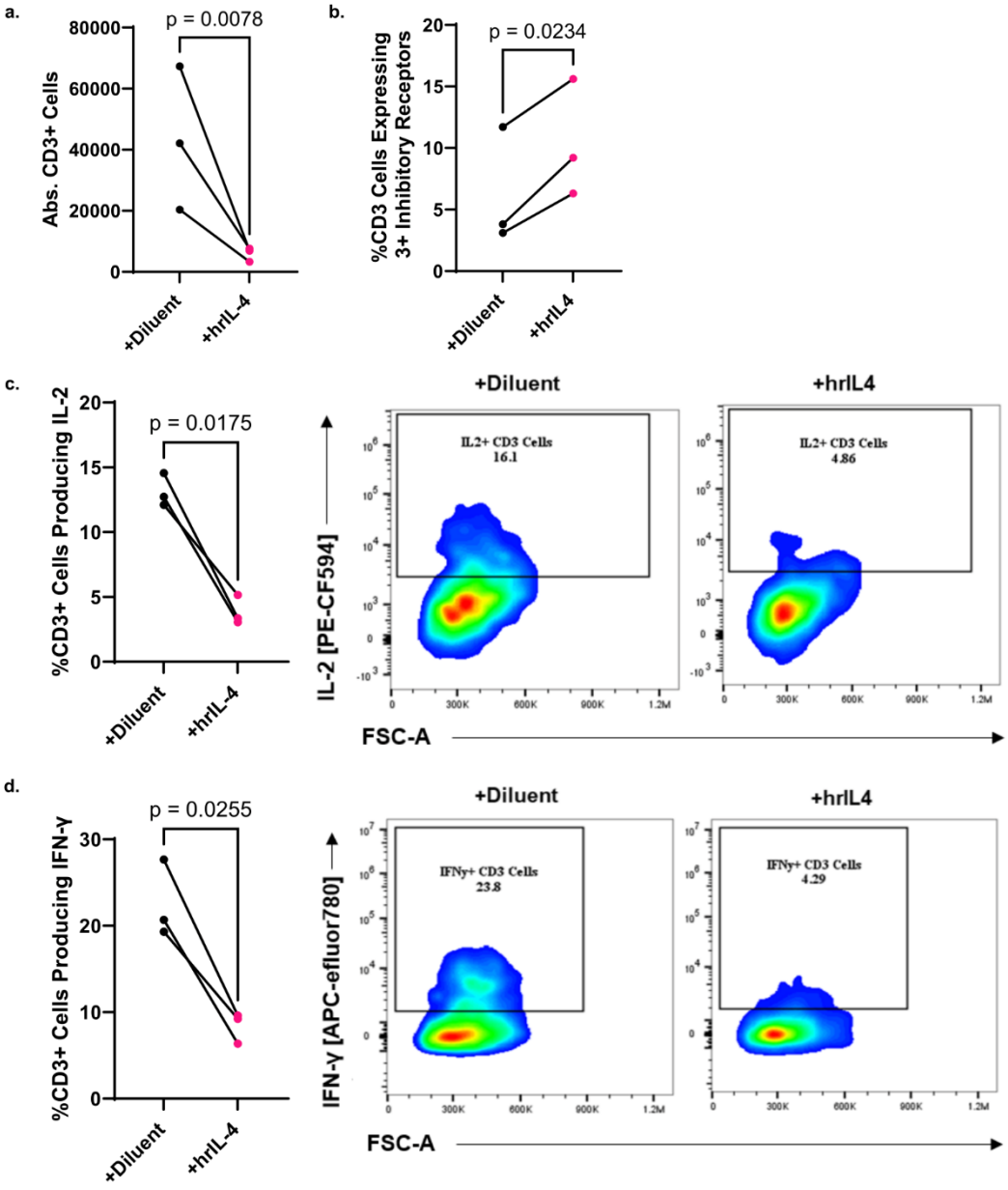

Supplementary Figure S16. **IL-4 causes CART cell dysfunction in CART cells targeting BCMA and containing a 4-1BB costimulatory domains (BCMA CART-BBζ). a-d.** BCMA CART-BBζ cells were chronically stimulated with OPM-2 tumor cells in the presence of either

20ng/mL hrIL-4 or diluent from Day 8 to Day 22 of the in vitro model for exhaustion. **a.** Absolute count of $CD3^+$ cells after Day 22 CART cells were co-cultured with OPM-2 tumor cells at a 1:1 E:T ratio for five days (Paired two-sided t-test, average of two technical replicates for three biological replicates). **b.** The percent of $CD3^+$ cells producing three or more inhibitory receptors on Day 22 as determined with flow cytometric detection of CD3, PD-1, CTLA-4, TIM-3, and LAG-3 (Paired two-sided t-test, average of two technical replicates for three biological replicates). **c-d.** Line graphs and representative flow plots showing the percent of $CD3^+$ cells producing IL-2 and IFN-γ as determined by intracellular staining and flow cytometry after Day 22 CART cells were co-cultured with OPM-2 cells at a 1:5 E:T ratio for four hours (Paired two-sided t-test, average of two technical replicates for three biological replicates). Source data are provided as a Source Data file.

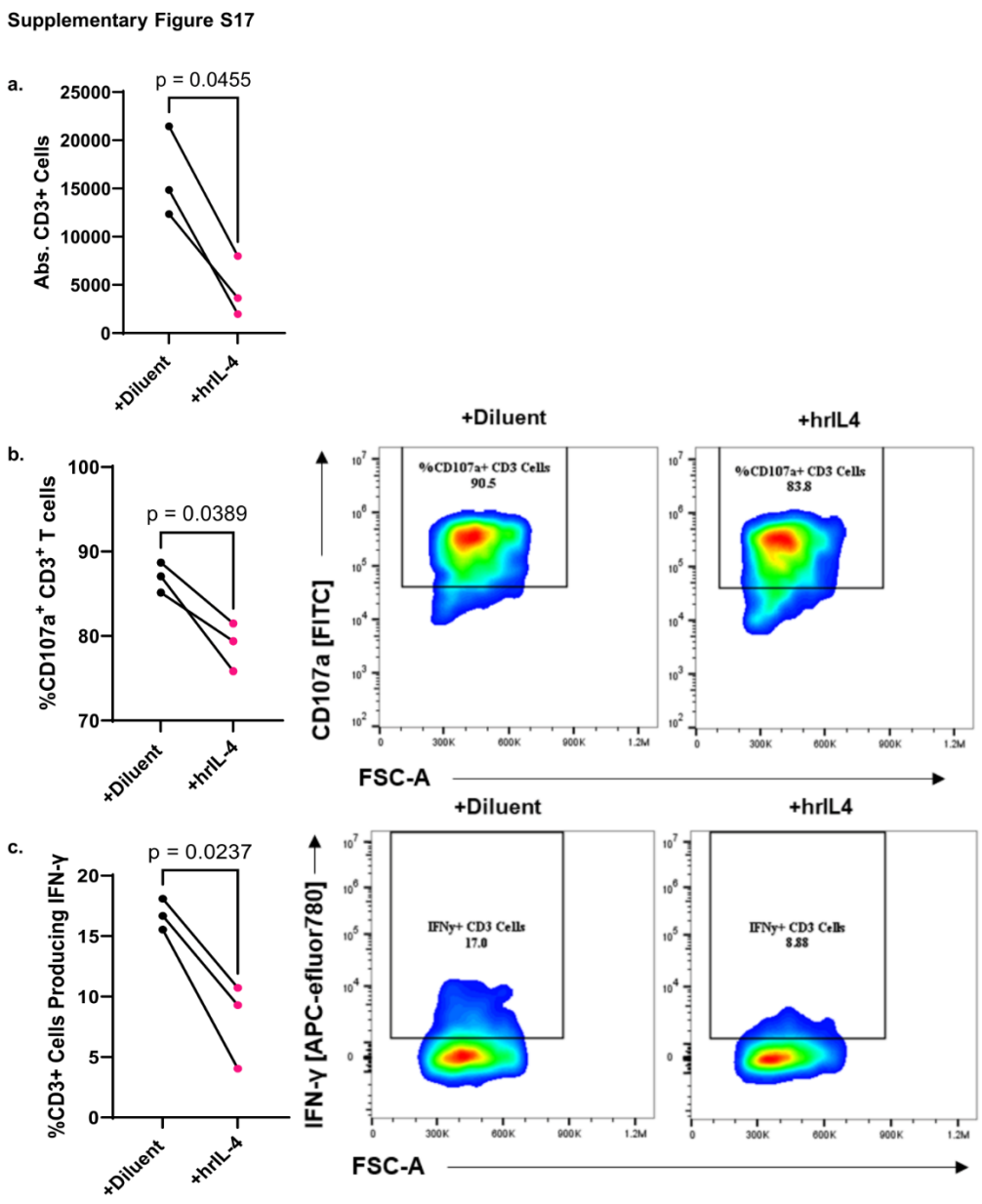

Supplementary Figure S17. **IL-4 causes CART cell dysfunction in CART cells targeting CS1 and containing a CD28 costimulatory domain (CS1 CART-28ζ). a-c.** CS1 CART-28ζ cells were chronically stimulated with OPM-2 tumor cells in the presence of either 20ng/mL hrIL-4 or diluent from Day 8 to Day 22 of the in vitro model for exhaustion. **a.** Absolute count of $CD3^+$ cells after Day 22 CART cells were co-cultured with OPM-2 tumor cells at a 1:1 E:T ratio for five days (Paired two-sided t-test, average of two technical replicates for three biological replicates). **b.** Line

graph and representative flow plots showing the percent of $CD3^+$ cells expressing CD107a as determined with flow cytometry after Day 22 CART cells were co-cultured with OPM-2 cells at a 1:5 E:T ratio for four hours (Paired two-sided t-test, average of two technical replicates for three biological replicates) **c.** Line graph and representative flow plots showing the percent of $CD3^+$ cells producing IFN-γ as determined by intracellular staining after Day 22 CART cells were co-cultured with OPM-2 cells at a 1:5 E:T ratio for four hours (Paired two-sided t-test, average of two technical replicates for three biological replicates). Source data are provided as a Source Data file.

Supplementary Figure S18

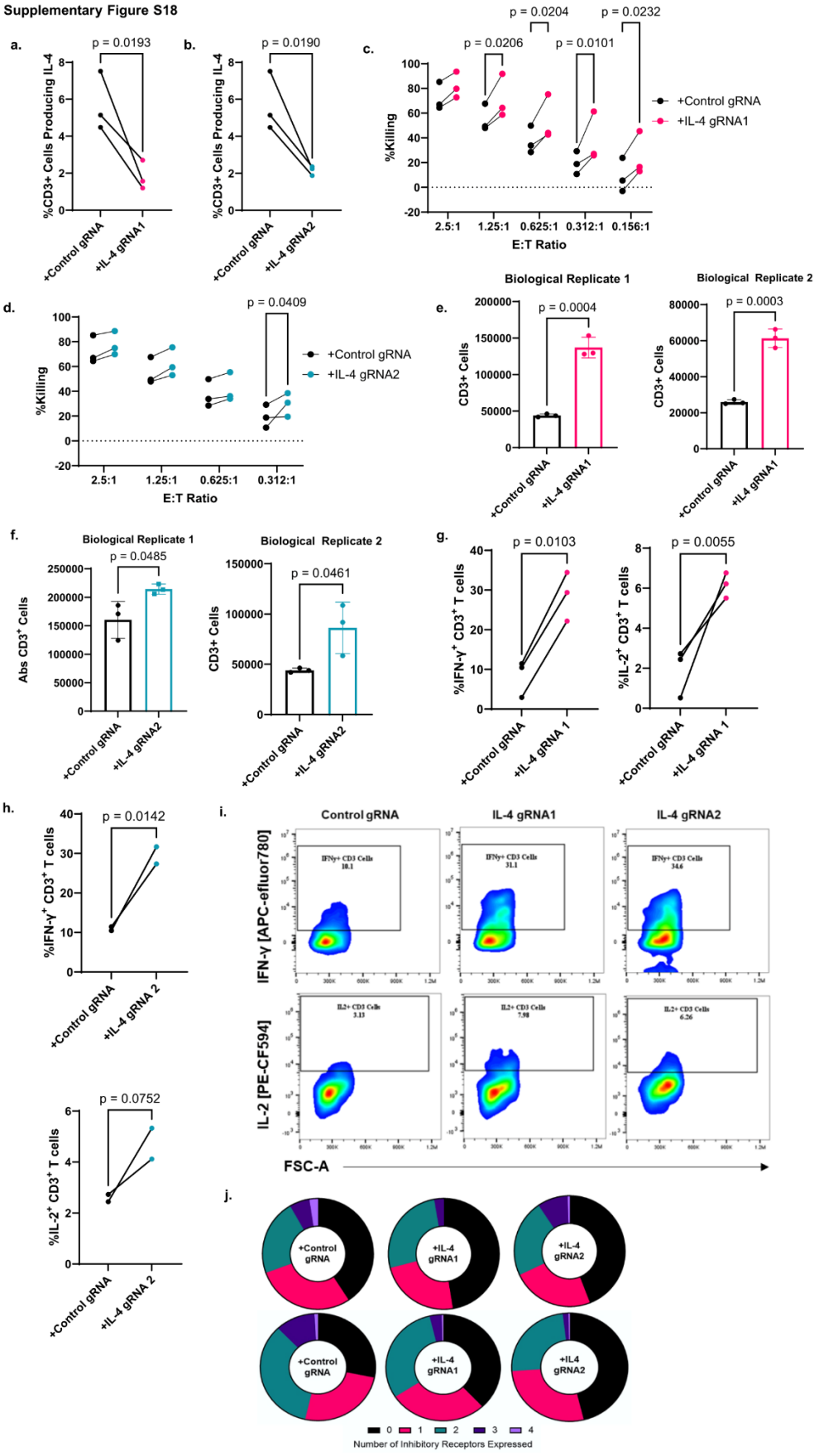

Supplementary Figure S18. **IL-4 knockdown reduces signs of exhaustion in CART19-28ζ cells. a-j.** During CART cell production, CART19-28ζ cells were transduced with a lentiCRISPRv2 plasmid containing a gRNA targeting IL-4 (gRNA1 or gRNA2) or a non-targeting gRNA (Control gRNA). **a-b.** The production of IL-4 by Day 8 CART19-28ζ cells as determined by intracellular staining after co-culturing CART cells with JeKo-1 tumor cells at a 1:5 E:T ratio for four hours (Paired two-sided t-test, average of two technical replicates for three biological replicates). **c-d.** Percent killing as measured with bioluminescent imaging after Day 8 CART19-28ζ cells were co-cultured with luciferase^{+} JeKo-1 cells at various E:T cell ratios for 48 hours (Paired two-way ANOVA, average of two technical replicates for three biological replicates). **e-f.** The absolute CD3^{+} count as determined by flow cytometry after Day 15 CART cells were co-cultured with JeKo-1 cells at a 1:1 E:T ratio for 5-days (Unpaired two-sided t-test, plots from individual biological replicates, three technical replicates, mean +/- SD). **g-i.** Line graphs and representative flow plots showing the production of effector cytokines such as IFN-γ and IL-2 as determined through intracellular staining after Day 15 CART cells were co-cultured with JeKo-1 cells at a 1:5 E:T ratio for four hours (Paired two-sided t-test, average of two technical replicates for each biological replicate). **j.** Circle graph depicting the percent of CD3^{+} cells expressing multiple inhibitory receptors (0 – black, 1 – pink, 2- green, 3 – dark purple, 4 – light purple) on Day 15 as determined by flow cytometric staining for CD3, PD-1, CTLA-4, TIM-3, and LAG-3 (Circle plots from two biologic replicates). Source data are provided as a Source Data file.

Supplementary Figure S19

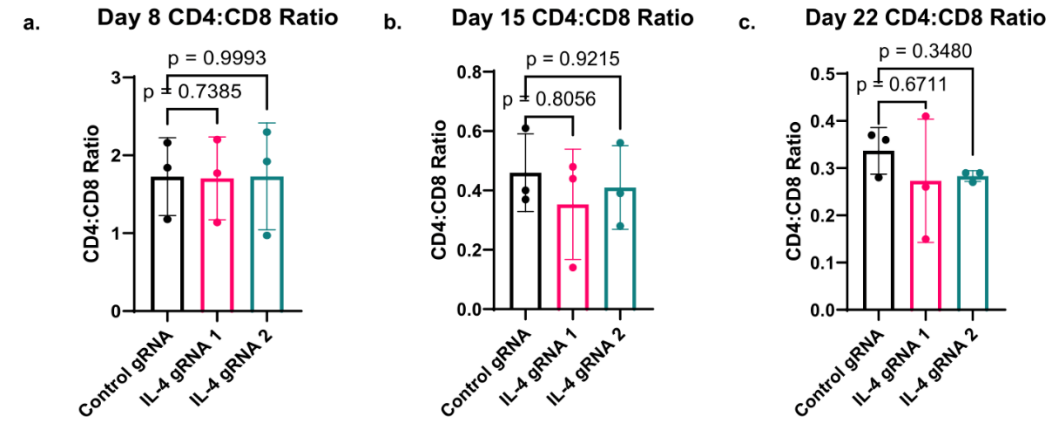

Supplementary Figure S19. **CRISPR/Cas9 knockout of IL-4 does not skew the CD4:CD8 ratio at baseline or following chronic stimulation. a-c.** The ratio of CD4:CD8 cells at Day 8, Day 15, and Day 22 of the in vitro model for exhaustion in CART19-28ζ cells transduced with a CRISPR/Cas9 virus containing either a non-targeting gRNA (Control gRNA) or a gRNA targeting IL-4 (One-way ANOVA, average of two technical replicates for three biological replicates, mean +/- SD). Source data are provided as a Source Data file.

Supplementary Figure S20

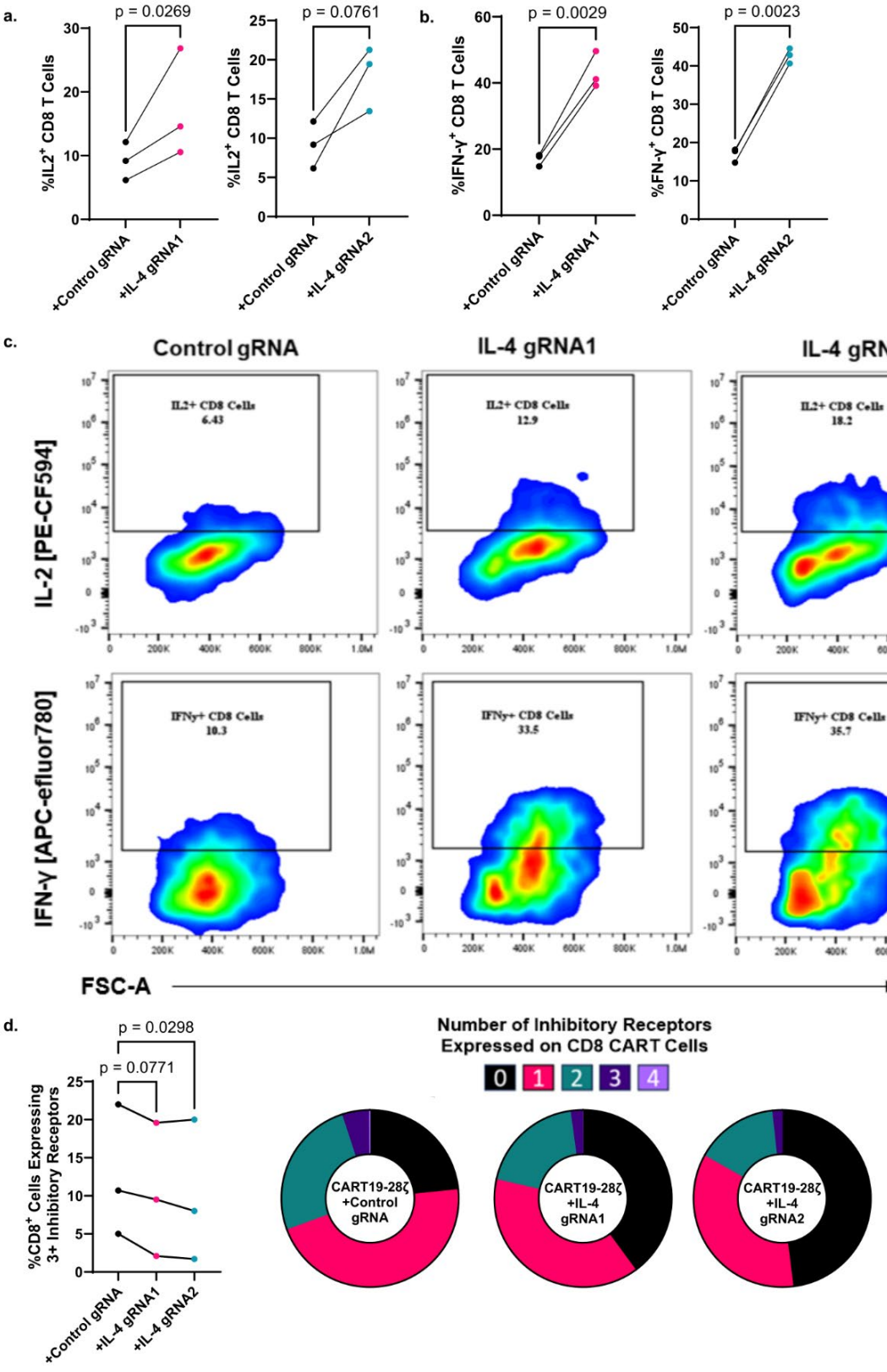

Supplementary Figure S20. **IL-4 knockdown reduces signs of exhaustion in CD8$^+$ CART19-28ζ cells. a-c.** Line graphs and representative flow plots showing the production of effector cytokines such as IL-2 and IFN-γ by CD8$^+$ CART cells. Determined through intracellular staining after Day 15 CART cells were co-cultured with JeKo-1 cells at a 1:5 E:T ratio for four hours (Paired two-sided t-test, average of two technical replicates for each biological replicate). **d.** Line graph and circle graphs depicting the percent of CD8$^+$ cells expressing multiple inhibitory receptors (0 – black, 1 – pink, 2- green, 3 – dark purple, 4 – light purple) on Day 15 as determined by flow cytometric staining for CD3, PD-1, CTLA-4, TIM-3, and LAG-3 (One-way ANOVA, average of two technical replicates for three biological replicates, circle plots from one representative biological replicate). Source data are provided as a Source Data file.

Supplementary Figure S21

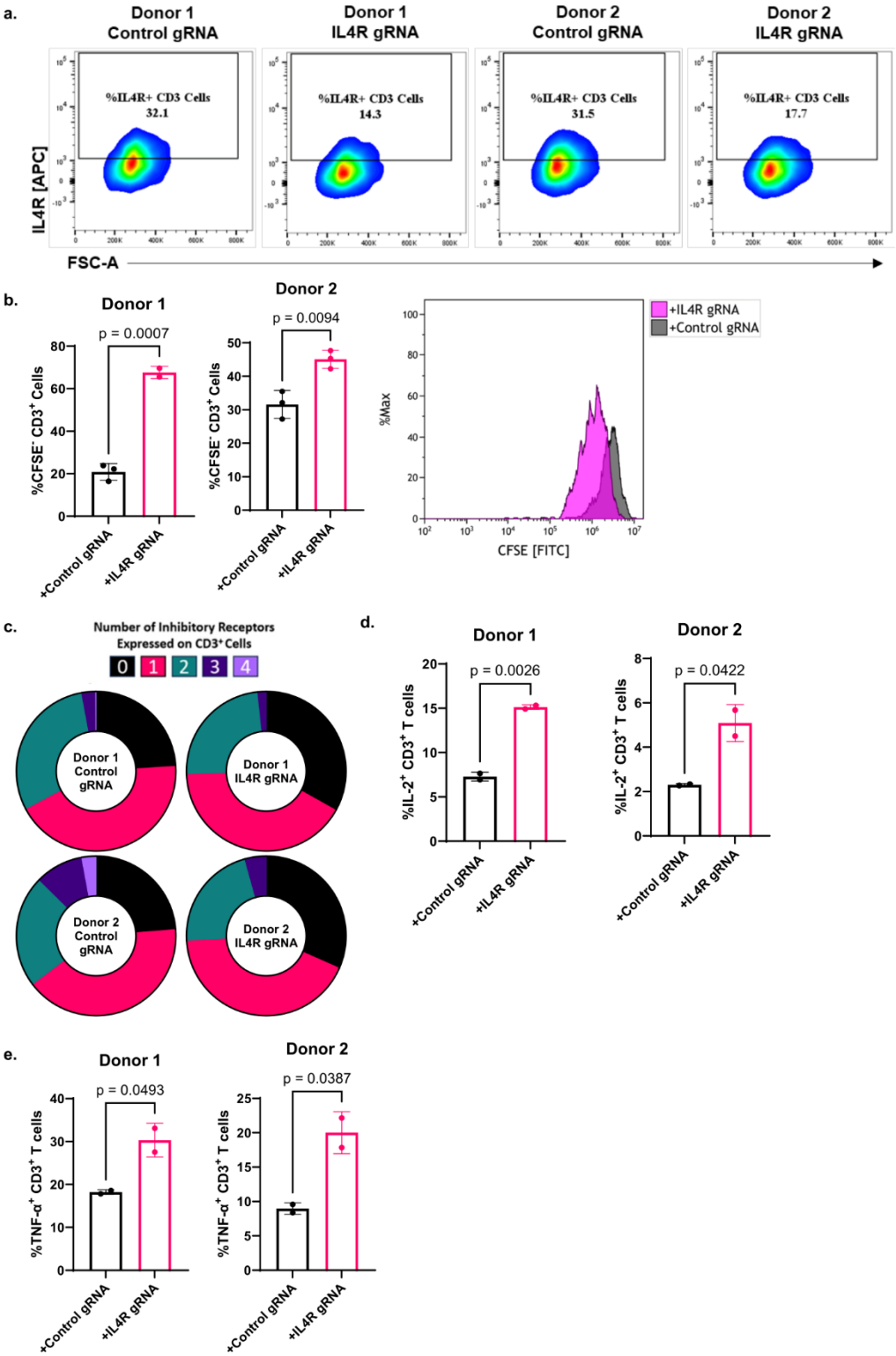

Supplementary Figure S21. **IL4R knockdown reduces signs of exhaustion in CART19-28ζ cells. a-e.** During CART cell production, CART19-28ζ cells were transduced with a lentiCRISPRv2 plasmid containing a gRNA targeting IL4R or a non-targeting gRNA (Control gRNA). **a.** Representative flow plots from two biological replicates (donors) showing the expression of IL4R on Day 8 CART19-28ζ cells. **b.** Bar plots and representative histogram showing the change in the percent of $CFSE^-$ CART cells when CFSE stained Day 22 CART cells were co-cultured with JeKo-1 tumor cells at a 1:1 E:T ratio for 5 days. (Unpaired two-sided t-test, plots from individual biological replicates, three technical replicates, mean +/- SD). **c.** Circle graphs depicting the percent of $CD3^+$ cells expressing multiple inhibitory receptors (0 – black, 1 – pink, 2- green, 3 – dark purple, 4 – light purple) on Day 22 as determined by flow cytometric staining for CD3, PD-1, CTLA-4, TIM-3, and LAG-3 (Circle plots from two biologic replicates). **d-e.** Bar graphs showing the production of IL-2 and TNF-α by $CD3^+$ CART cells as determined through intracellular staining after Day 22 CART cells were co-cultured with JeKo-1 cells at a 1:5 E:T ratio for four hours (Unpaired two-sided t-test, plots from individual biological replicates, two technical replicates, mean +/- SD). Source data are provided as a Source Data file.

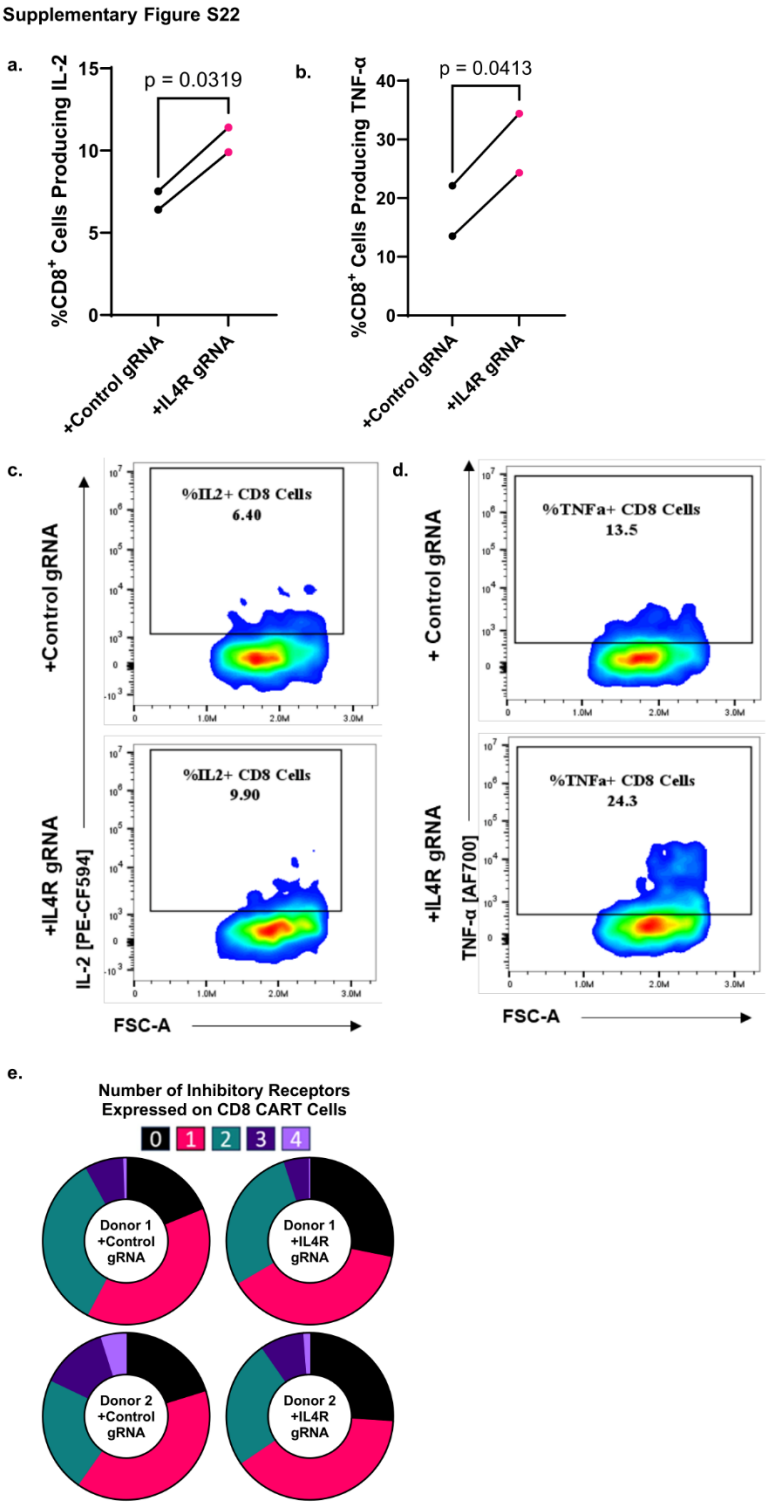

Supplementary Figure S22. **IL4R knockdown reduces signs of exhaustion in CD8$^+$ CART19-28ζ cells. a-e.** During CART cell production, CART19-28ζ cells were transduced with a

lentiCRISPRv2 plasmid containing a gRNA targeting IL4R or a non-targeting gRNA (Control gRNA). **a-d.** Line and representative flow plots showing the production of IL-2 and TNF-α by $CD8^+$ CART cells as determined through intracellular staining after Day 22 CART cells were co-cultured with JeKo-1 cells at a 1:5 E:T ratio for four hours (Paired two-sided t-test, average of two technical replicates for two biological replicates). **e.** Circle graphs depicting the percent of $CD8^+$ cells expressing multiple inhibitory receptors (0 – black, 1 – pink, 2- green, 3 – dark purple, 4 – light purple) on Day 15 as determined by flow cytometric staining for CD3, CD8, PD-1, CTLA-4, TIM-3, and LAG-3. Source data are provided as a Source Data file.

Supplementary Figure S23

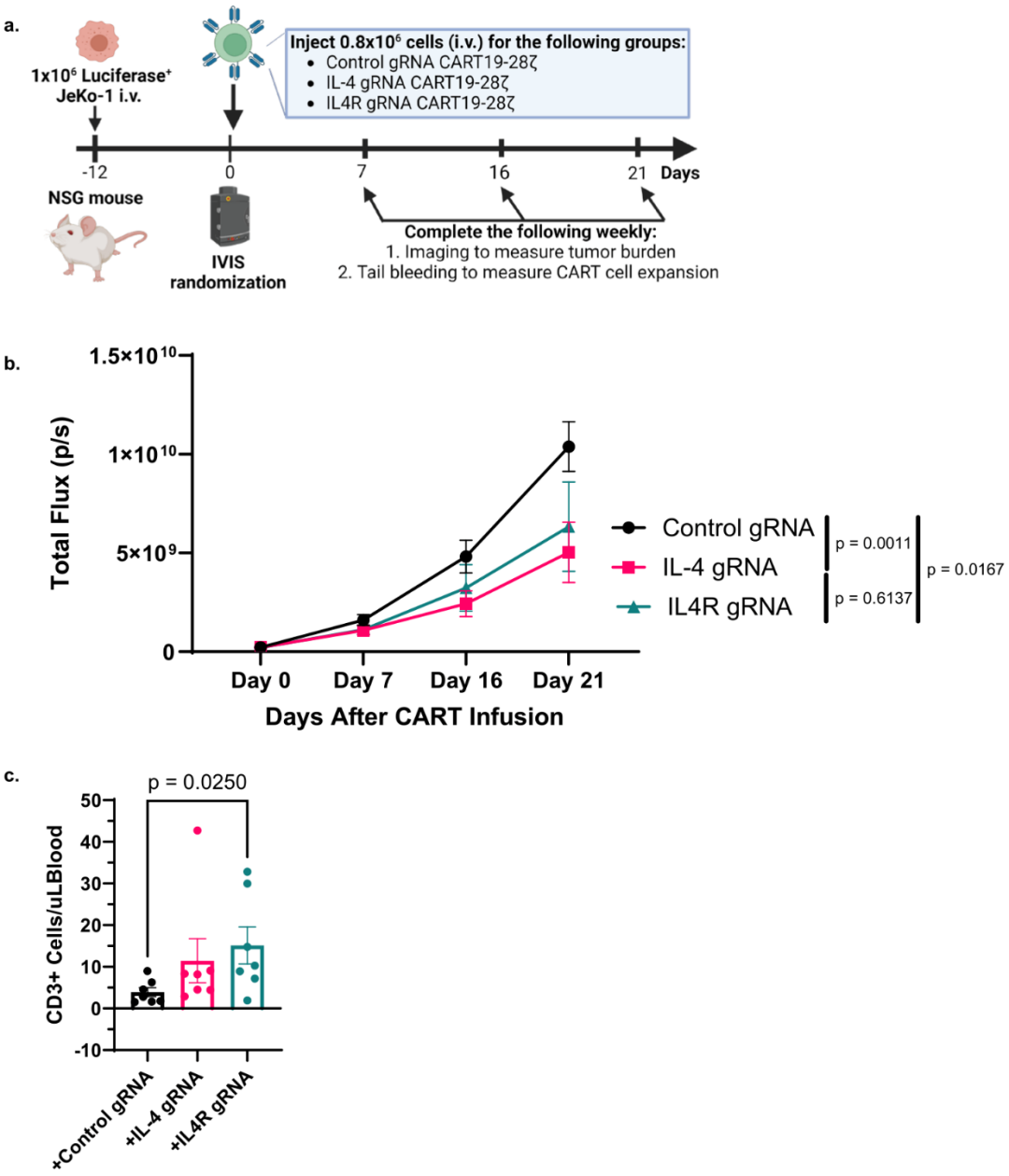

Supplementary Figure S23. **IL-4 and IL4R knockdown improves CART19-28ζ cell activity in a JeKo-1 xenograft model. a.** Schematic depicting an in vivo mantle cell lymphoma xenograft mouse model to induce stress in CART19 cells (Supplementary Figure S23a was created with BioRender.com released under a Creative Commons Attribution-NonCommercial-NoDerivs 4.0 International license). **b.** Tumor burden over time in a mantle cell lymphoma xenograft mouse

model as determined by bioluminescence imaging of the luciferase^{+} tumor (Two-way ANOVA, n=7 mice per group, mean +/- SEM) **c.** Absolute human CD3^{+} cells per µL of peripheral blood as determined by flow cytometry on Day 19 of a mantle cell lymphoma xenograft mouse model (One-way ANOVA, n=7 mice per group, mean +/- SEM). Source data are provided as a Source Data file.

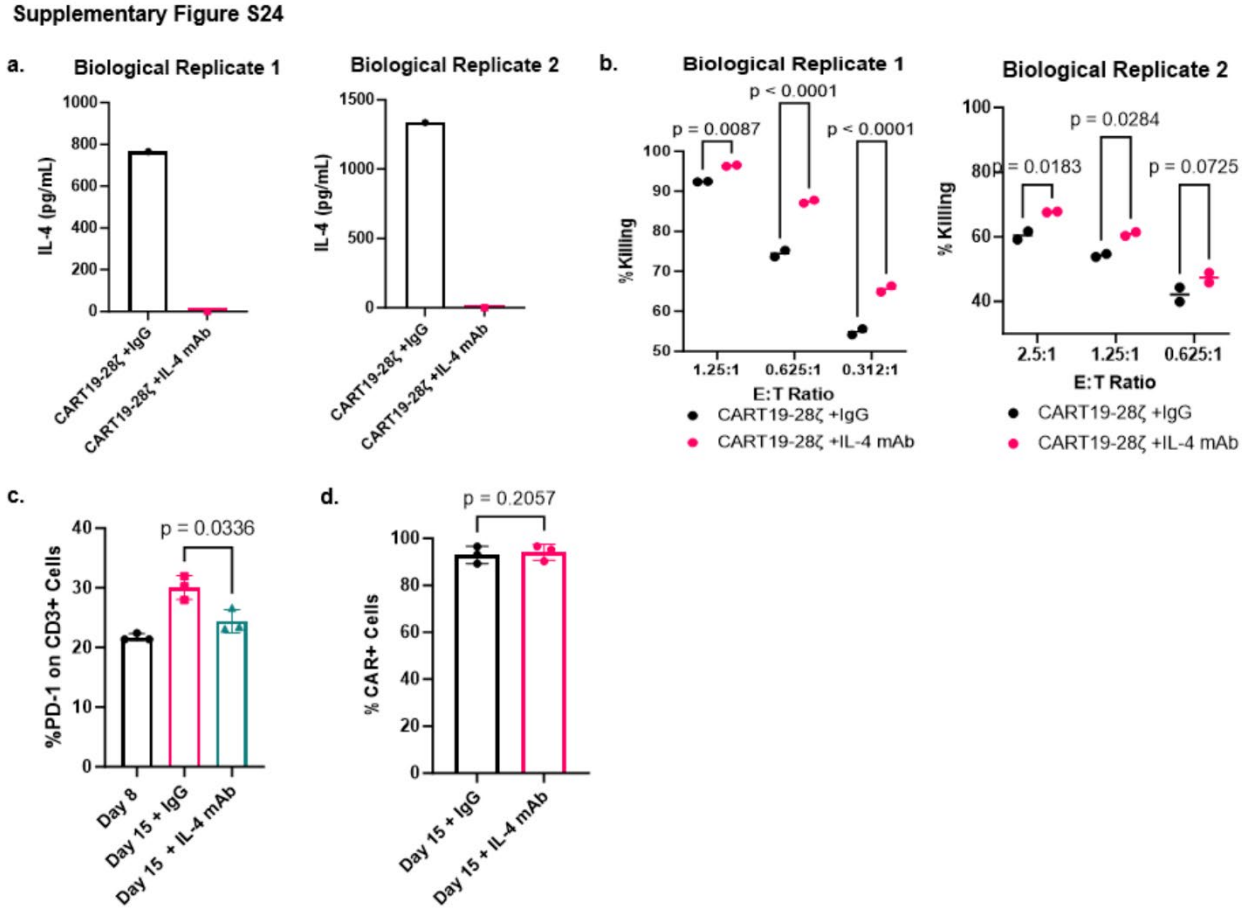

Supplementary Figure S24. **The effect of IL-4 neutralization with a mAb on CART19-28ζ function in vitro. a.** The concentration of IL-4 in the supernatant after CART19-28ζ cells were co-cultured with JeKo-1 target cells at a 1:1 E:T ratio for three days in the presence of either 10µg/mL IL-4 mAb or IgG control antibody (results from two biological replicates). **b.** Cytotoxicity of CART19-28ζ cells that were co-cultured with luciferase^{+} JeKo-1 targets cells at various E:T ratios in the presence of either 10µg/mL IL-4 mAb or

IgG control antibody for 48 hours (Two-way ANOVA, results from two biological replicates, two technical replicates per biological replicate). **c.** The percent of $CD3^+$ cells that are positive for PD-1 at Day 8 and Day 15 after being chronically stimulated with JeKo-1 cells in the presence of either 10μg/mL IL-4 mAb or IgG control antibody from Day 8 to Day 15 (One-way ANOVA, average of two technical replicates for three biological replicates, mean +/- SD). **d.** The percent of CAR^+ cells following chronic stimulation (Day 15) in the presence of 10μg/mL IL-4 mAb or IgG control antibody as determined by ProteinL staining for flow cytometry. (Paired two-sided t-test, average of two technical replicates for three biological replicates, mean +/- SD). Source data are provided as a Source Data file.

Supplementary Figure S25

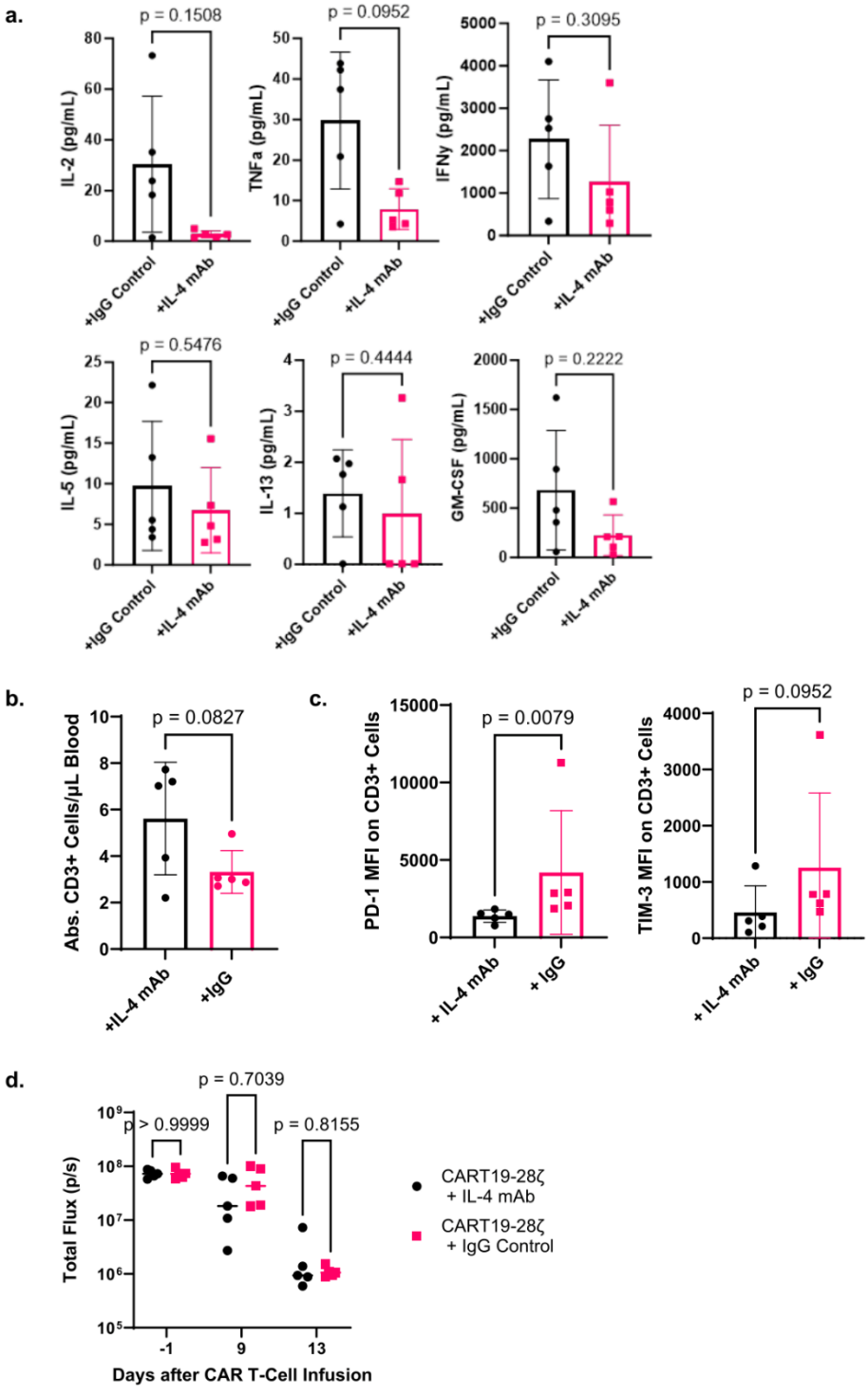

Supplementary Figure S25. **The effect of IL-4 neutralization on CART19-28ζ efficacy in stress and low tumor burden mantle cell lymphoma xenograft mouse models. a.** Individual plots

showing the concentration of detected cytokines on week two of the mantle cell lymphoma xenograft stress mouse model treated with Day 8 CART19-28ζ cells in combination with either 10mg/kg IL-4 mAb or IgG control antibody. (two-sided t-test, n=5 mice per group, mean +/- SD). **b.** CART cell expansion in vivo as determined by absolute $hCD45^{+}CD3^{+}$ count by flow cytometry per µL of blood two weeks following CART cell infusion in a low tumor burden mantle cell lymphoma xenograft mouse model (two-sided t-test, n=5 mice per group, mean +/- SD). **c.** The mean fluorescence intensity of the inhibitory receptors PD-1 and TIM-3 by flow cytometry on CART cells in mice treated with either CART19-28ζ cells and 10mg/kg IL-4 mAb or CART19-28ζ cells and 10mg/kg IgG control antibody on week two of a low tumor burden mantle cell lymphoma xenograft mouse model (two-sided t-test, n=5 mice per group, mean +/- SD). **d.** Tumor progression as measured with bioluminescence imaging of $luciferase^{+}$ JeKo-1 cells in a low tumor burden mantle cell lymphoma xenograft mouse model where the mice were treated with CART19-28ζ cells in combination with either 10mg/kg IL-4 mAb or IgG control antibody (Two-way ANOVA with n=5 mice per group). Source data are provided as a Source Data file.

Supplementary Figure S26

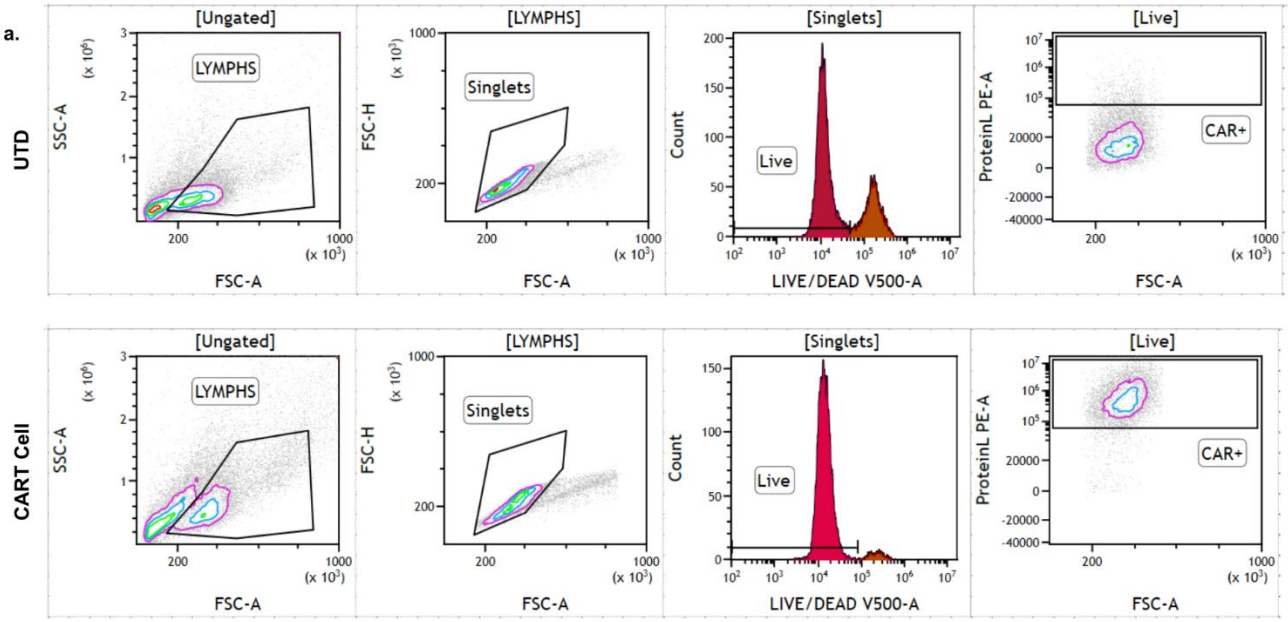

Supplementary Figure S26. **Representative flow plot for the determination of CAR percentage. a.** Representative flow plots showing the determination of CAR positivity. Positive gating for ProteinL PE is determined through staining of untransduced (UTD) T cells with ProteinL PE.

Supplementary Figure S27

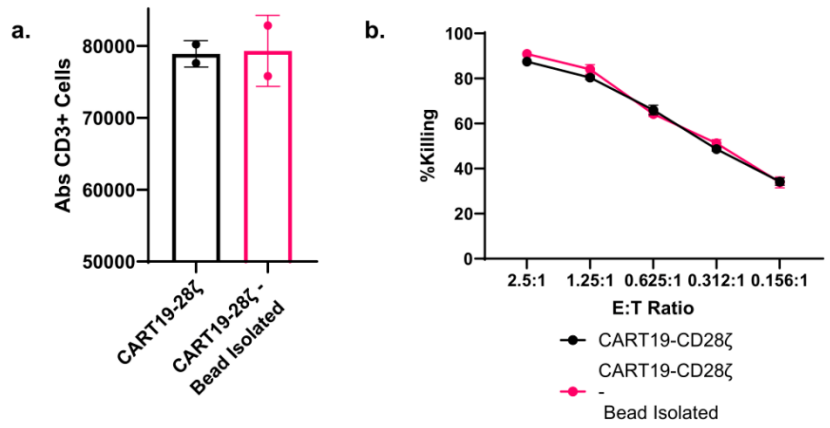

Supplementary Figure S27. **The use of CD4$^+$ and CD8$^+$ beads to separate CART cells from co-culture does not impact functionality. a.** Absolute CD3$^+$ cell count as determined by flow cytometry after culturing CART19-28ζ cells that had either undergone bead separation or not, with JeKo-1 target cells at a 1:1 E:T cell ratio for 5-days (One biological replicate and two technical replicates, mean +/- SD). **b.** Cytotoxicity of CART19-28ζ cells that either underwent bead separation or did not before culture with luciferase$^+$ JeKo-1 target cells at various E:T ratios for 48 hours (One biological replicate and two technical replicates). Source data are provided as a Source Data file.

Supplementary Figure S28

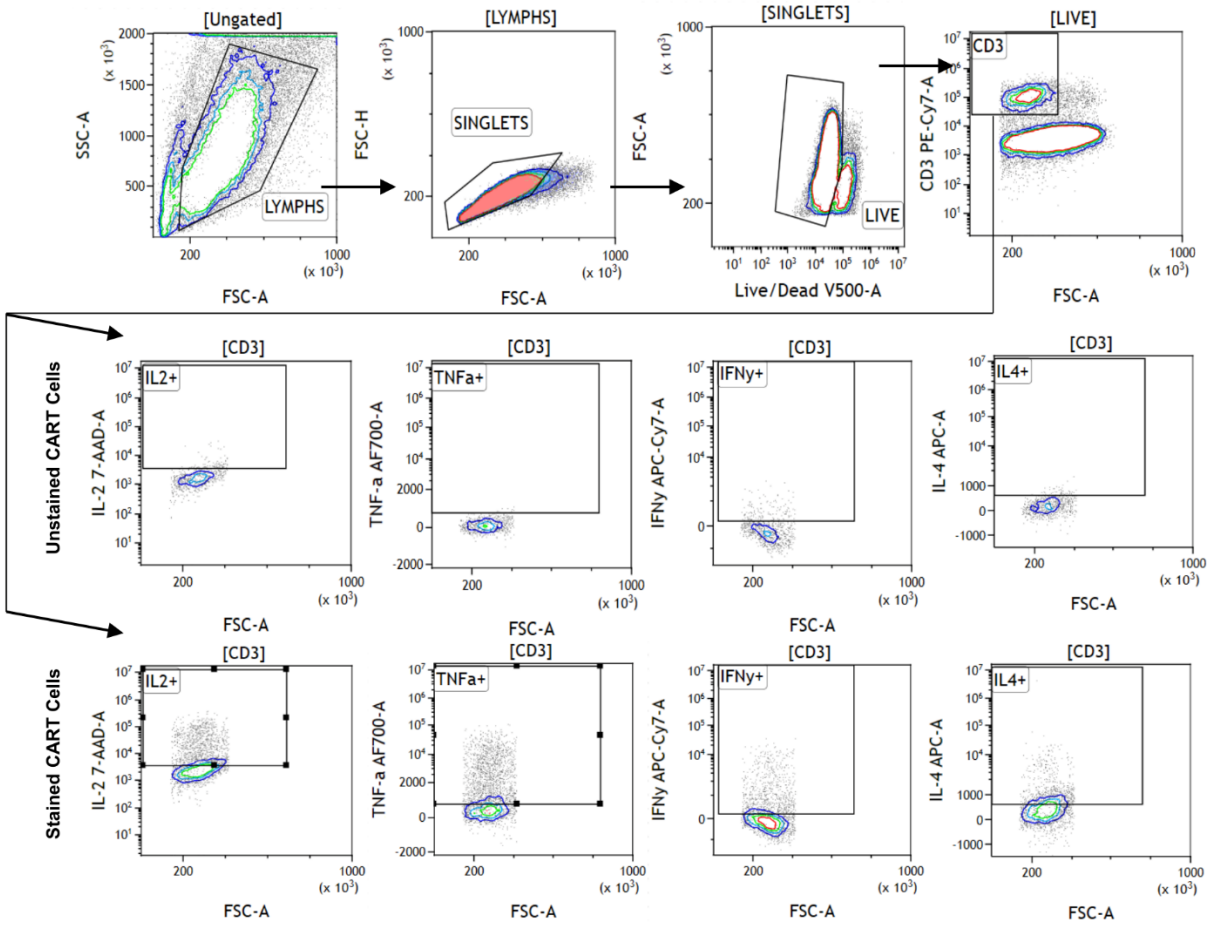

Supplementary Figure S28. **Example gating strategy used to determine the percentage of T cells producing cytokines.** Unstained CART cells were used to determine positive gating for cytokines of interest in the stained CART samples. (Figures generated in Kaluza, contour with outliers, the colors represent density with the least dense being black, then dark blue, then light blue, then green, and then red).

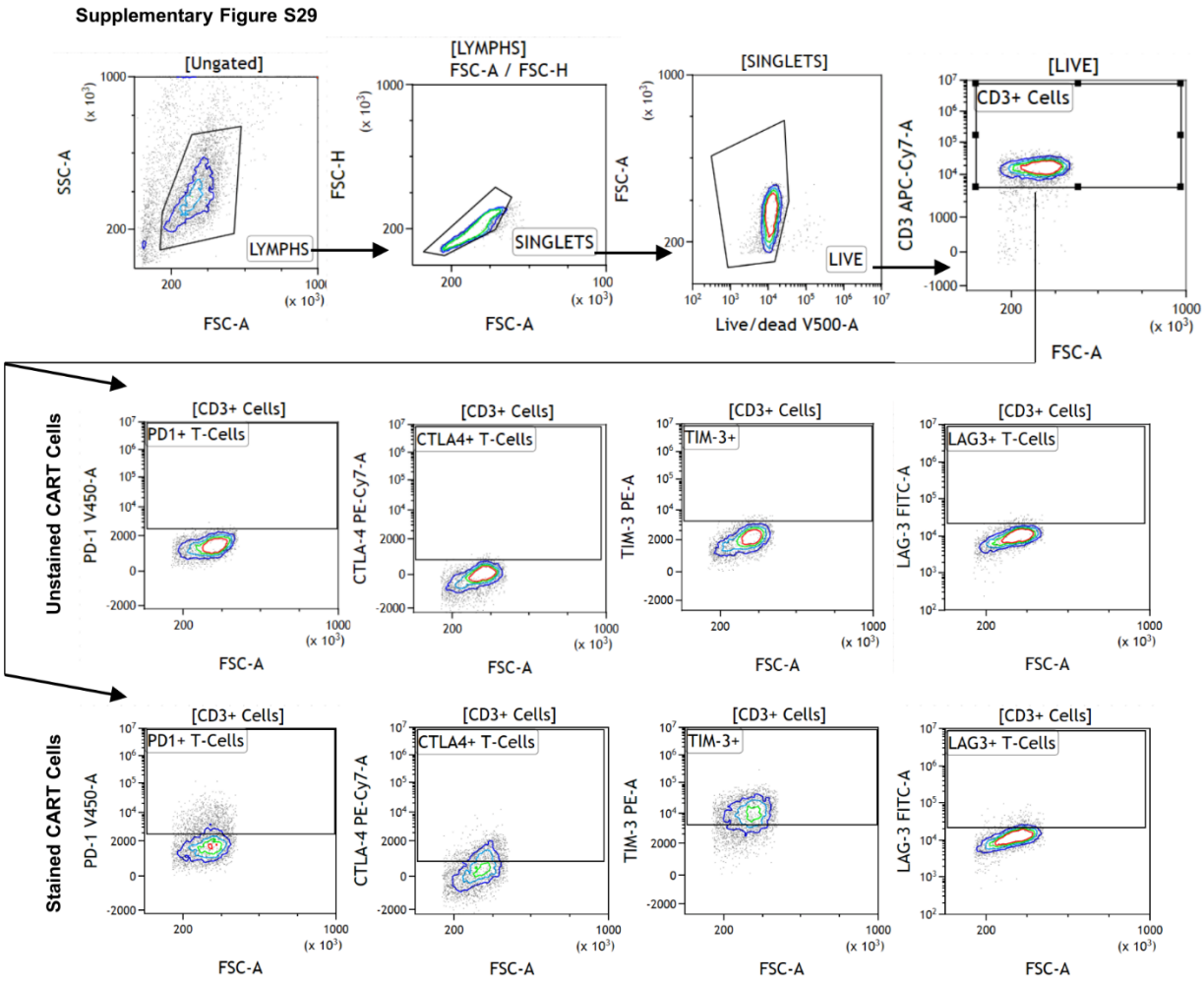

Supplementary Figure S29. **Example gating strategy used to determine the percentage of T cells positive for inhibitory receptors.** Unstained CART cells were used to determine positive gating for each inhibitory receptor (PD-1, CTLA-4, TIM-3, and LAG-3) in the stained CART samples. (Figures generated in Kaluza, contour with outliers, the colors represent density with the least dense being black, then dark blue, then light blue, then green, and then red).

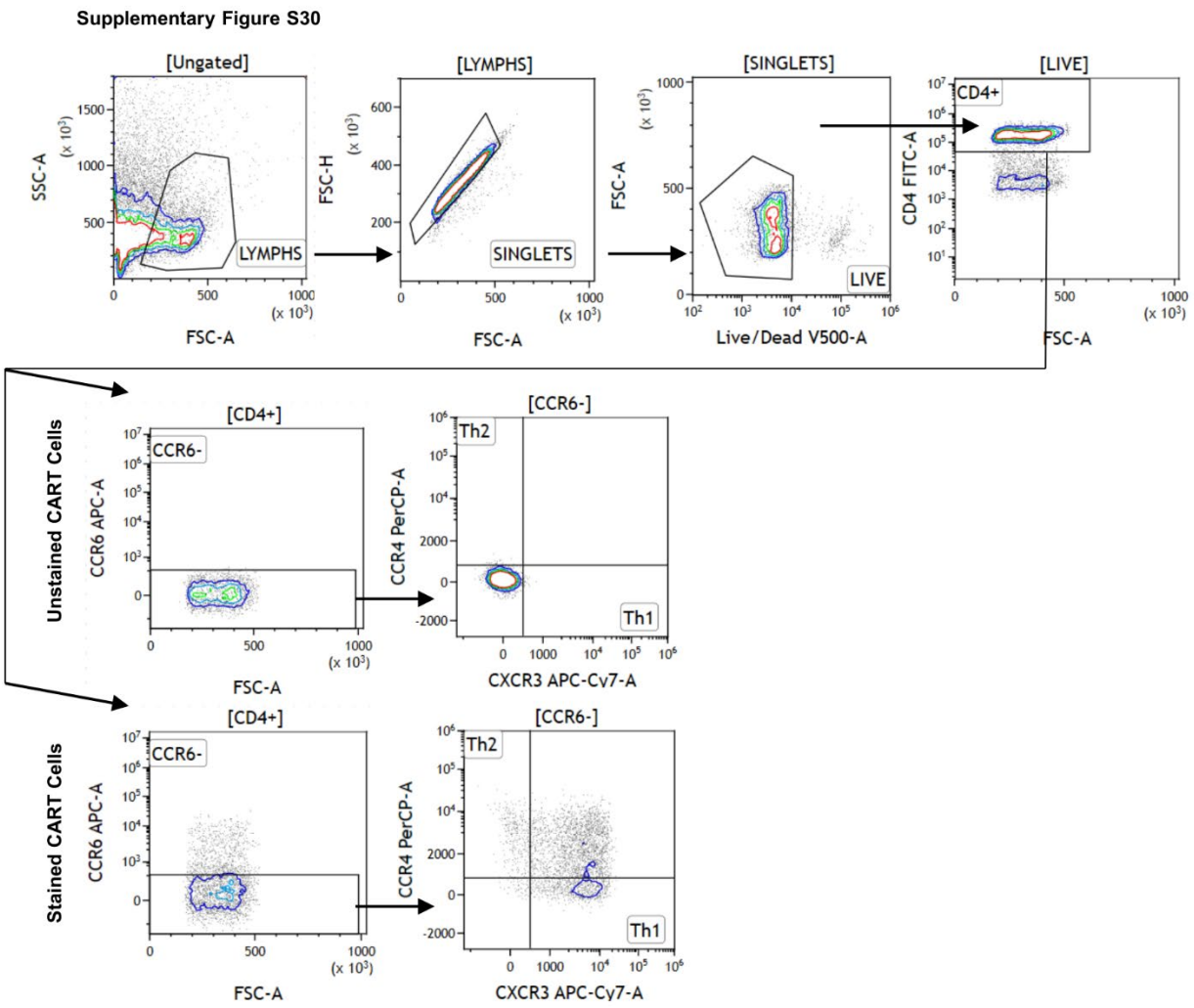

Supplementary Figure S30. **Example gating strategy used to determine the percentage of Th1 or Th2 CD4$^+$ T cells.** Unstained CART cells were used to determine positive gating in the stained CART samples. (Figures generated in Kaluza, contour with outliers, the colors represent density with the least dense being black, then dark blue, then light blue, then green, and then red). Th1 cells are defined as CD4$^+$CCR6$^-$CCR4$^-$CXCR3$^+$ and Th2 cells are defined as CD4$^+$CCR6$^-$CCR4$^+$CXCR3$^-$.

Supplementary Figure S31

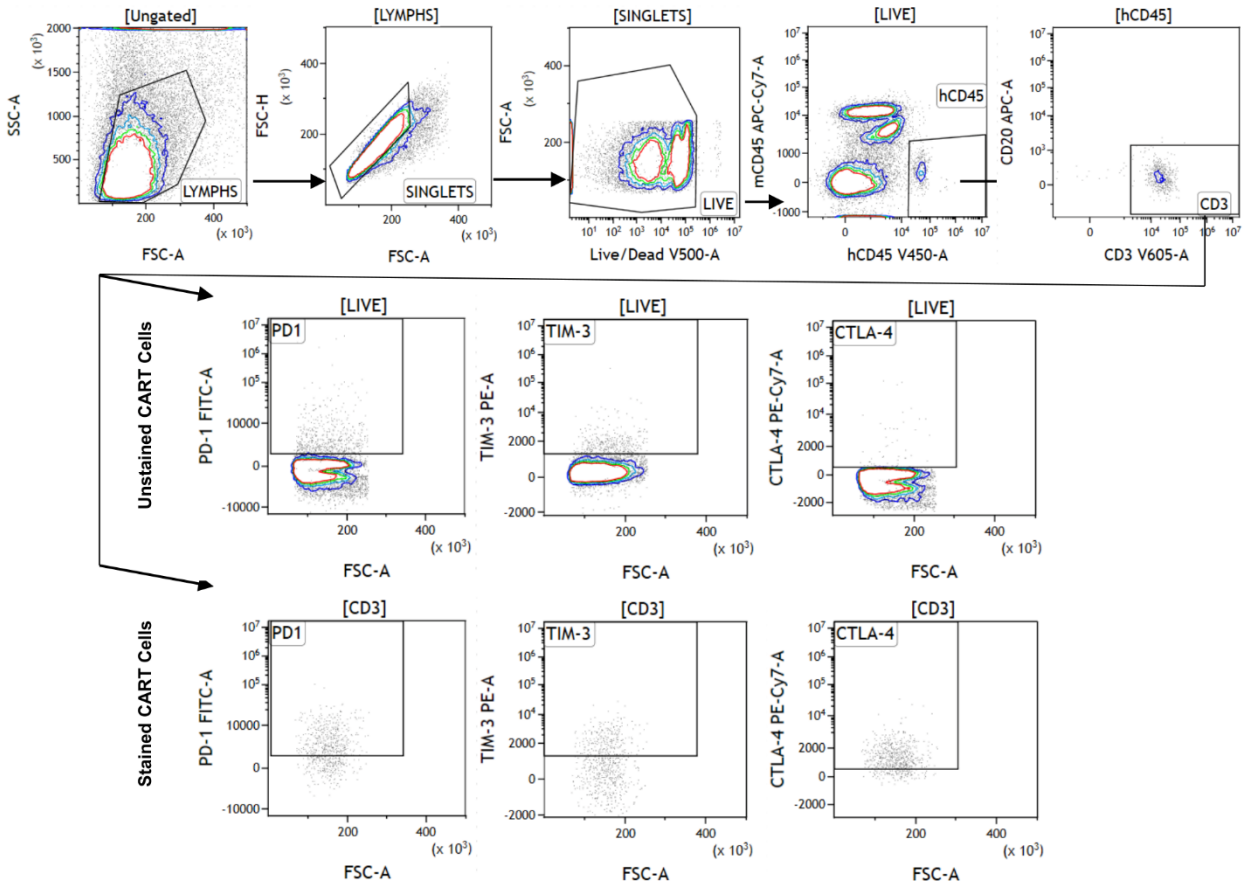

Supplementary Figure S31. **Example gating strategy used to evaluate the expansion of human T cell expansion in NSG mice.** Unstained CART cells were used to determine positive gating in the stained CART samples. (Figures generated in Kaluza, contour with outliers, the colors represent density with the least dense being black, then dark blue, then light blue, then green, and then red).